CrossMark

Magnetotelluric Studies for Hydrocarbon and Geothermal Resources: Examples from the Asian Region

Prasanta K. Patro[1] ⓘ

Abstract Magnetotellurics (MT) and the other related electrical and electromagnetic methods play a very useful role in resource exploration. This review paper presents the current scenario of application of MT in the exploration for hydrocarbons and geothermal resources in Asia. While seismics is the most preferred method in oil exploration, it is, however, beset with several limitations in the case of sedimentary targets overlain by basalts or evaporate/carbonate rocks where the high-velocity layers overlying the lower velocity layers pose a problem. In such cases, MT plays an important and, in some cases, a crucial role in mapping these potential reservoirs because of significant resistivity contrast generally observed between the basalts and the underlying sedimentary layers. A few case histories are presented that typically illustrate the role of MT in this context. In the case of geothermal exploration, MT is known to be highly effective in deciphering the target areas because of the conductivity structures arising from the presence and circulation of highly conductive fluids in the geothermal target areas. A few examples of MT studies carried out in some of the potential areas of geothermal significance in the Asian region are also discussed. While it is a relatively favorable situation for application of EM and MT methods in the case of exploration of the high-enthalpy region due to the development of well-defined conceptual models, still the low-enthalpy regions need to be understood well, particularly because of more complex structural patterns and the fluid circulation under relatively low-temperature conditions. Currently, a lot of modeling in both geothermal and hydrocarbon exploration is being done using three-dimensional techniques, and it is the right time to go for integration and three-dimensional joint inversion of the geophysical parameters such as resistivity, velocity, density, from MT, electromagnetics (EM), seismics and gravity.

Keywords Geothermal · Hydrocarbon · Magnetotellurics · Electromagnetics · Asia

✉ Prasanta K. Patro
  patrobpk@ngri.res.in

[1] CSIR-National Geophysical Research Institute, Uppal Road, Hyderabad 500007, India

1 Hydrocarbon Resources

1.1 Introduction

The natural hydrocarbons (oil and gas) are associated with some specific geological conditions and structures. The three different units that constitute a hydrocarbon target are (1) the source rock, the rock formation that provides hydrocarbon generating conditions; (2) the reservoir rock that helps to store the generated hydrocarbons; and (3) the trap, the geological structure that facilitates preservation of hydrocarbons. Using different geophysical techniques, we detect the favorable geological structures, while direct detection of hydrocarbons is still a difficult task.

The main objective of any hydrocarbon exploration program is to identify and image these units, viz. reservoir rock, structure, or trap and its configuration/boundary. Identification of reservoir boundary is very important because cost-effective drilling can be done only with the prior information about the position and structure of the reservoir unit. Besides the common structures like anticlines, others like reef barriers and salt domes are also important structures where hydrocarbons may get accumulated. The primary goal of any geophysical study, particularly seismics, the most common and preferred geophysical tool in oil exploration, is to image these sediments and the associated structural features. While seismics is known to be a highly successful geophysical tool in exploring a wide range of hydrocarbon targets, in some cases, particularly when such sedimentary structures of hydrocarbon potential are overlain by higher velocity volcanic cover as in the case of sub-trappean Mesozoic sediments in India, seismic methods become less effective in mapping such sub-trappean sediments (Krishna et al. 1999; Ziolkowski et al. 2003). The hydrocarbon exploration will thus become difficult with seismic method alone if the favorable geological structures for hydrocarbons lie beneath such high velocity or heterogeneous overlying layers. In such special geological and structural environments, magnetotellurics (MT) together with other electromagnetic methods, like controlled-source EM (CSEM) or transient EM (TEM), play a crucial role since they are highly effective and offer valuable inputs that could be integrated with seismic results. MT has an additional advantage of probing deeper subsurface sections compared to other EM methods and provides a general view of the potential areas for further exploration. Controlled source EM methods generate an electric current that flows in both horizontal and vertical directions facilitating detection of high resistive layers and, under favorable conditions, they provide a possibility for direct detection of hydrocarbons (Ziolkowski et al. 2002; Unsworth 2005). Hoversten et al. (2006) have developed a new joint inversion procedure to estimate reservoir parameters directly by using both seismic amplitude variation with angle of incidence (AVA) data and marine controlled-source electromagnetic (CSEM) data.

Another parameter particularly important to be estimated in hydrocarbon exploration is the porosity of the reservoir rocks since the quality of reservoir may be assessed by the value of its porosity. The reservoir will be more productive and efficient if the rock is more porous and permeable. The application of EM methods including MT in hydrocarbon exploration has a great advantage indeed, in that the resistivity values with in a resistivity model can be used to estimate porosity which in turn facilitates an efficient analysis of the reservoir quality.

MT studies were carried out for hydrocarbon exploration programs in various countries round the globe, and several case histories may be found in earlier reviews (Meju 2002; Strack 2014). The review by Meju (2002) on the geoelectromagnetic exploration for natural resources deals with the basic understanding of the geological models of resource

targets, and development of conceptual geoelectromagnetic exploration models followed by case studies and outstanding challenges in exploration. Meju (2002) made a review of groundwater, geothermal, metallic ore bodies apart from hydrocarbon exploration. Strack (2014) discussed more a practical approach, focusing on the techniques including joint inversion of MT and seismic data that is commonly used for exploration in the industry. He presented some of the interesting case studies dealing with surface-to-borehole experiments, EM time-lapse measurements and borehole EM.

During the last two decades, application of MT technique gained significant momentum in Asia as well. Figure 1 presents the map of Asia showing the countries for which MT studies for hydrocarbon and geothermal exploration are discussed in the present review. Extensive MT studies are being carried out in China, for various exploration and tectonic studies and the average yearly coverage amounts to as much as 14,000 MT stations in China alone (He et al. 2010a). Electromagnetic profiling technique (CEMP) and time and frequency electromagnetic (TFEM) were developed and deployed in combination with MT for exploration of hydrocarbons in different geological scenarios (He et al. 2010a, b). In the topographically challenging regions such as Kuche and Taxinan of Tarim Basin, western Qaidam Basin, northern margin of Qaidam Basin, western margin of Ordos Basin of China, and 3D continuous electromagnetic profiling (CEMP) surveys proved to be very useful (He et al. 2010a, b). Three-dimensional CEMP studies can image potential structures and confirm the results obtained from the seismic data. Similarly, the TFEM has been applied to several regions in China for target evaluation and oil prediction (Dong and Zhao 2008). Another interesting study was carried out in the Tarim Basin, western China, where the apparent resistivity from TFEM studies and the induced polarization (IP) anomalies were used to detect potential oil-bearing zones (He et al. 2010a).
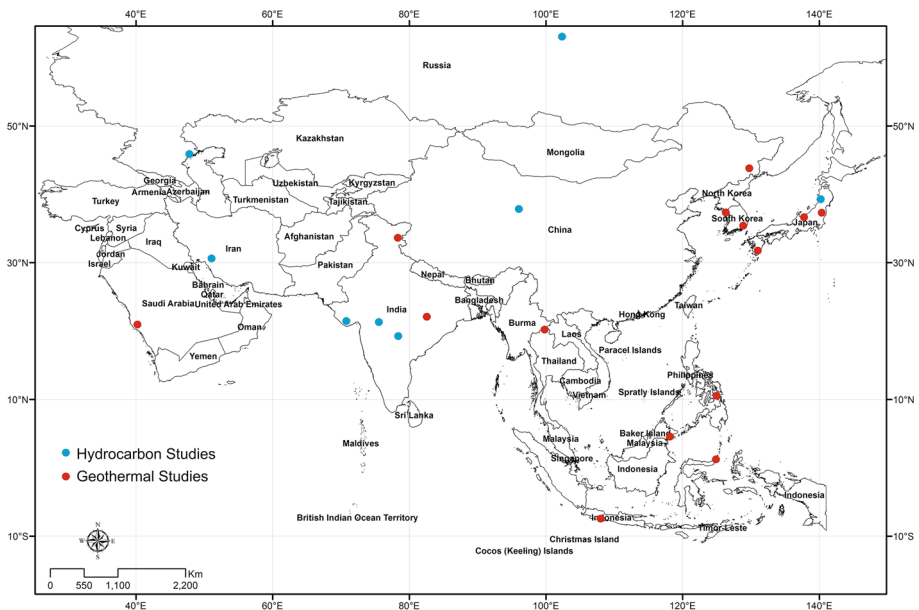
Fig. 1 Map of Asia showing the countries for which MT studies for hydrocarbon and geothermal exploration are discussed in this review

MT was used successfully in oil exploration in Iran where the Zagros zone is the main geological unit holding the reservoir systems of the oil fields (Mansoori et al. 2015, 2016; Sarvandani et al. 2017). In India, where sub-basalt imaging is the main challenge, MT is shown to be a very effective exploration tool for imaging sub-trappean sedimentary columns (Sarma et al. 1992, 1998a, b, c; Harinarayana et al. 2000b, 2003, 2009; Patro and Sarma 2007; Abdul Azeez et al. 2011; Pandey et al. 2008, 2009; Satpal et al. 2006; Patro et al. 2015a) and also in Japan where the subsurface is quite complex, having a basaltic layer overlain by carbonate rocks (Matsuo and Negi 1999; Mitsuhata et al. 1999). In Russia, the main problem in exploration is imaging of reef systems having halogeneous carbonates, and the MT deployment has provided several useful clues such as the geometry of terrigenous sediments, barrier reef, halogen structures and carbonate massif (Berdichevsky et al. 2015).

Though MT is being used extensively for hydrocarbon exploration, the results/case studies are not publicly available due to several restrictions in industry. I shall present here results of some available examples of MT application from the Asian region to bring out its application potential in different complex lithological and structural environments as an individual tool as well as in combination with controlled-source electromagnetic techniques and other geophysical methods, particularly seismics. The case studies indeed suggest that in hydrocarbon exploration, in particular, an integrated approach using MT, in a combination of other EM methods, seismic and well log data is a highly effective approach to investigate complex geological situations like mapping of sub-basalt sediments. Further, application of 3D MT modeling for exploration of oil and gas is highly effective and useful as illustrated through synthetic examples (for, e.g., see Zhang et al. 2014) and also as seen from some of the case studies (Matsuo and Negi 1999; Mansoori et al. 2016).

2 Some Examples of MT Application for Hydrocarbons (Oil and Gas) from Asia

2.1 Sehqanat Oil Field, Iran

More than 95% of oil fields in Iran are located in the Zagros zone. Extensive MT studies are being carried out in this zone (Mansoori et al. 2015, 2016). The Sehqanat oil field
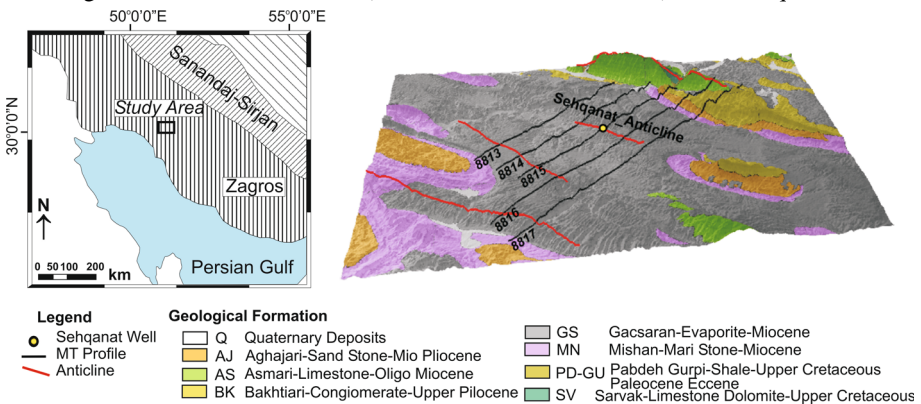
Fig. 2 The location of the study region which lies in the Zagros sedimentary column (left). Geological map of the study region (left). The geological map of the study region is shown to the right. The parallel lines marked in black color are the MT profiles, and the red lines are the anticline axis (Mansoori et al. 2016)

(SOF) located in the SW of Iran belongs to the Zagros sedimentary zone (Fig. 2). The Zagros range is located along the tectonic boundary between the Arabian and Eurasian plates (Takin 1972). Numerous NW–SE-trending fold structures were formed as a result of collision along this boundary (Alan 1969). The Sehqanat anticline is one of the such gentle and moderate-sized structures of the Zagros basin in which Asmari Formation serves as the major reservoir for hydrocarbons. This has been investigated recently using MT (Mansoori et al. 2015, 2016).

The Asmari limestone formation constituting the reservoir rock in the Zagros zone is one of the giant reservoirs in the world, and 85% of total crude oil of Iran is exploited from this Asmari Formation (Rezaie and Nogole Sadat 2004). But in the case of Sehqanat oil field (SOF) region, the Asmari Formation is overlain by a heterogeneous formation of Gachsaran evaporates having high seismic velocity (4500 m/s) compared to the underlying Asmari Formation (Fig. 2). A 2D reflection seismic survey was conducted in SOF along five profiles, but low-quality, discontinuous and spurious seismic events were observed in most parts of the sections. In contrast to the seismic velocity section, the electrical resistivity from well log data showed relatively well-defined steplike change from about 1 Ωm in Gachsaran Formation to nearly 100 Ωm in Asmari Formation (Fig. 3). Because of this sharp contrast in electrical resistivity and in view of the poor seismic data quality, MT was deployed for imaging the Asmari Formation and to identify and demarcate the reservoir.
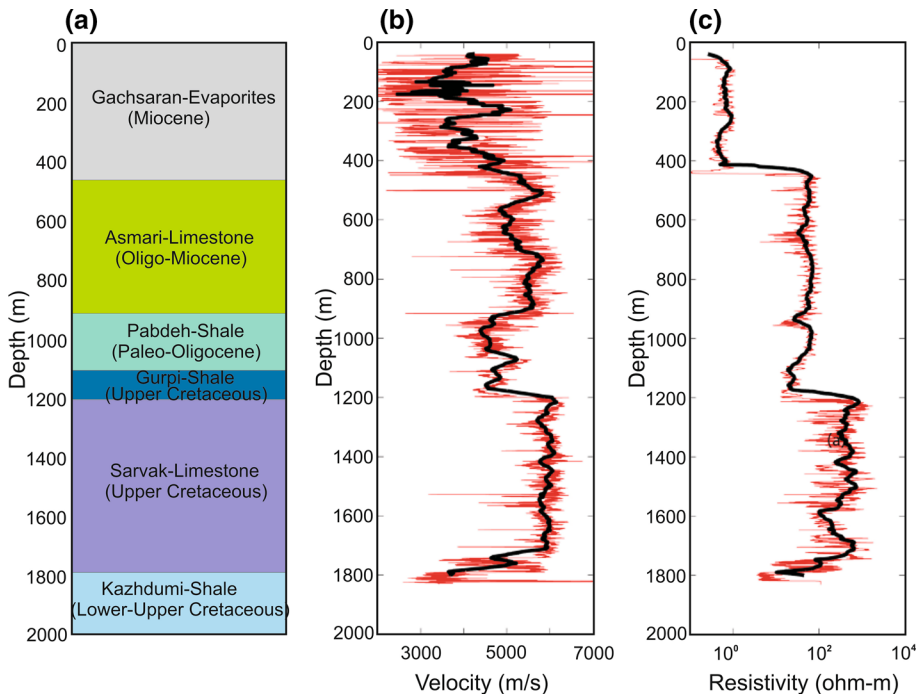
Fig. 3 Geological formations sequence (a), velocity (b) and resistivity logs (c) of Sehqanat well is presented (Mansoori et al. 2015). It may be noted that, while the velocity log shows significant inhomogeneity in the Gachsaran Formation, the resistivity logs present a uniform and well-defined resistivity contrast between the Gachsaran evaporites and Asmari Limestones

A high-resolution MT survey was carried out during 2013 by the National Iranian Oil Company (NIOC) along five SW–NE-trending parallel profiles, with a profile spacing of 300 m. MT data, in the period range of 0.003–1000 s, were acquired, from more than 600 sites, located along these profiles, using the remote reference methodology. In addition to MT, TEM data were also recorded at 400 locations mainly for carrying out the static shift correction of MT data. Two-dimensional inversion was carried out for TE, TM, TE + TM and DET (determinant data, $Z_{DET} = \sqrt{Z_{xx}Z_{yy} - Z_{xy}Z_{yx}}$) modes of data within the period range of 0.001–700 s.

The Sehqanat anticline could be resolved well on all the 2D resistivity sections as a resistive dome-shaped body located in the middle part of all the five MT profiles. Correlation of the resistivity models with the reflection seismic sections has further sharpened the boundary of the structure besides moderately reducing the ambiguities in the seismic interpretation. In a later study (Mansoori et al. 2016), 3D modeling of MT data was also done for the region and the anticline is imaged in the 3D model (Fig. 4).

2.2 Sub-Basalt Imaging in India

2.2.1 Saurashtra Peninsula

Exploration for hydrocarbons for the Mesozoic sediments in the Deccan trap covered areas in India remained a challenging problem for a long time. The Mesozoic sediments, known as potential hydrocarbon target formation, are believed to lie between the overlying Deccan basalts and the Precambrian basement below. Worldwide, Mesozoic sediments contain 50% of the world's oil reserves and 40% of gas reserves (Bois et al. 1982). In India, substantial Mesozoic sedimentation has taken place, the majority of which is believed to be hidden underneath thick layers of the Late Cretaceous Deccan basalts. The Deccan Trap volcanics besides fulfilling the thermal requisites for hydrocarbon maturation also provide
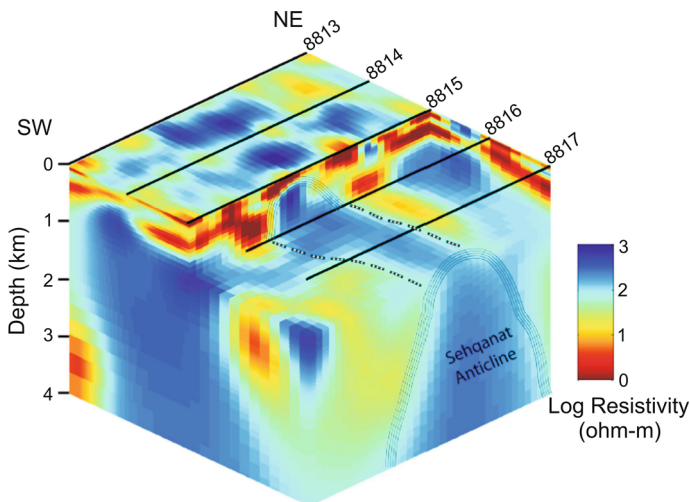

Fig. 4 Three-dimensional electrical model derived from the magnetotellurics (Mansoori et al. 2016), MT profiles are plotted on the top of the model. The high resistive dome-like features represents the Sehqanat anticline

favorable conditions for preserving the underlying Mesozoic strata and their hydrocarbons from exposure and erosion over a long period (Zutshi 1991).

Imaging of these sub-trappean sediments for hydrocarbon prospecting using conventional seismic methods is found to be highly complex and ambiguous, and for such a geological scenario MT and other electromagnetic techniques should serve as an effective tool as shown in the recent exploration efforts launched by the National Geophysical Research Institute (NGRI). The NGRI for the first time initiated experimental magnetotelluric studies during 1987–1990 along two N–S- and E–W-trending regional profiles cutting across the entire Saurashtra peninsula (Sarma et al. 1992). These studies have successfully delineated a thick sub-trappean sedimentary layer in the northern part of the Saurashtra peninsula. Later, Oil and Natural Gas Corporation Limited drilled a bore hole passing through the Deccan trap layer in Lodhika and the MT results correlated well with the bore hole section showing the sub-trappean sedimentary layer (see Figs. 5, 6). Impressed and encouraged by these results, Oil Industry Development Board (OIDB) and Oil and Natural Gas Corporation Limited (ONGC) came forward and funded a major project to NGRI for an integrated geophysical study of the entire Saurashtra region using MT, seismic, gravity and well log data. Under this program, broadband MT data were acquired at 600 sites covering the entire Saurashtra (Sarma et al. 1998a). The modeling of the data set led to the detection of a major Mesozoic sedimentary basin in the northwestern part of Saurashtra peninsula (Fig. 7). Besides this, detailed mapping of thickness variation pattern of Deccan trap as also the detection of several linear structural features interpreted as faults and volcanic plugs was also accomplished. Long-offset transient electromagnetic (LOTEM) studies were also carried out during late 1980s in the Saurashtra region (Strack and Pandey 2007). One-dimensional and 3D modeling studies of the LOTEM data also revealed the presence of the low resistive Mesozoic sediments sandwiched between more resistive basalt layers and the high resistive basement, which was later validated by drilling
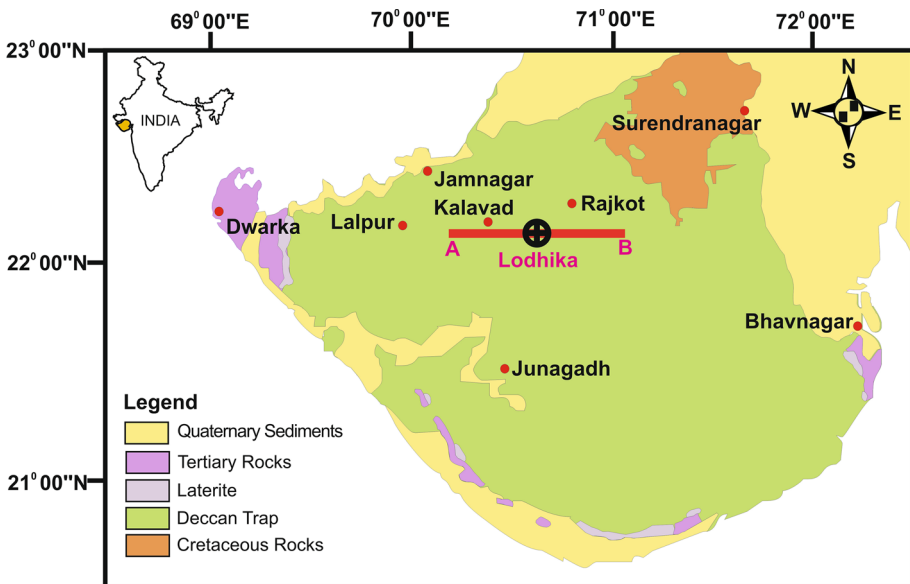
Fig. 5 Geological map of the Saurashtra region, India (modified after Merh 1995). Most part of Saurashtra is covered with Deccan Traps
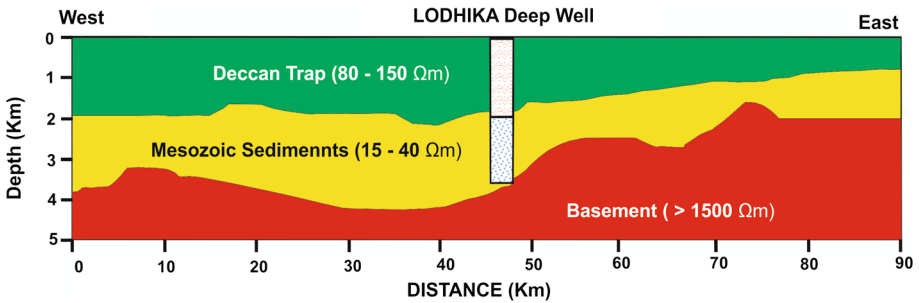
Fig. 6 Electrical section along the line AB cutting across the Lodhika Bore well (for location see Fig. 5). Deccan Trap thickness obtained from 1D MT modeling is quite consistent with drilling results (Harinarayana 2008)
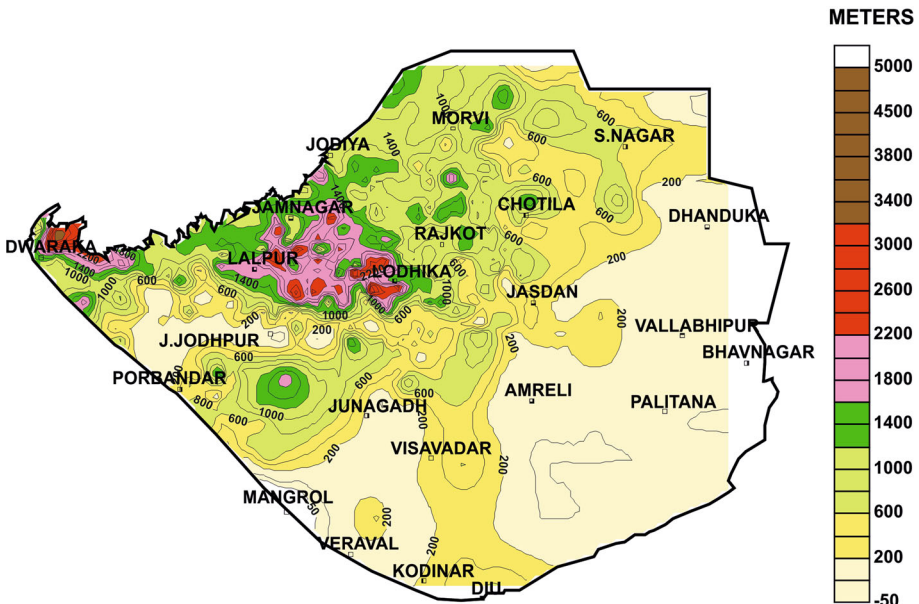
Fig. 7 Mesozoic sediment thickness map obtained from the integrated geophysical study (Sarma et al. 1992, 1998a; Singh and Arora 2008). Based on the sediment thickness map, a sub-trappean basin with a thick sedimentary column is delineated at the northwestern segment of Saurashtra. Mesozoic sediments are the source rock for hydrocarbon reserves (Bois et al. 1982)

results (Strack and Pandey 2007). Subsequent to the success of MT studies in Saurashtra, two more areas, viz. Narmada–Son zone and the Nagpur–Wardha regions, were covered by MT (Sarma et al. 1998b; Harinarayana et al. 2003, 2009) in combination with other geophysical methods.
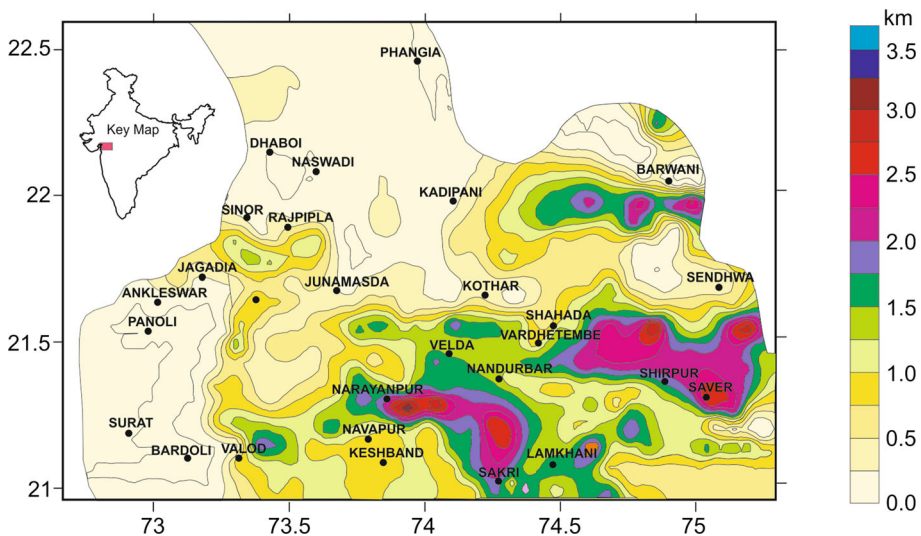
2.2.2 Narmada-Son Lineament Zone

Narmada–Tapti rift zone in Central India, covered by Deccan traps, is yet another important area, for hydrocarbon exploration of sub-trappean sediments. Magnetotelluric

data were acquired at more than 1000 MT stations in a grid pattern with site spacing of 5–8 km (Fig. 8). To get a broad outline of the possible Mesozoic sediment thickness variations below basalt cover of the Narmada–Tapti region, based on 1D inversion results a contour map for sediment thickness was prepared (Harinarayana et al. 2003, 2009). The results showed that the sediment thickness varied over a wide range, from few tens of meters to as much as 3.5 km (Fig. 8). Two features were identified as quite prominent, i.e., a thick (2–3 km) sedimentary basin toward the north of Shirpur and another basin extending from Narayanpur to Sakri with sediment thickness of about 2.5 km (Fig. 8).

2.3 Yurihara Oil Field, Japan

The Yurihara oil and gas field, located on the southern edge of Akita Prefecture, NE Japan (see Fig. 9a), is yet another area with a complex shallow subsurface section characterized by a volcanic cover, hindering the effective use of seismic studies. The subsurface section in the study area consists of layers of Chokai volcanics at the top overlying the Nishime, Sasaoka, Upper Tentokuji, Funakawa, Onnagawa, Nishikurosawa and Yashiozawakawa Formations which are basically carbonate rocks (Ozawa et al. 1988; Ichinoseki 1984). The well log data (Mitsuhata et al. 1999) show the Nishikurosawa Basalt Group (NBG) of Miocene age in which oil and gas reservoirs were found to occur at depths ranging from 1.5 to 2.0 km. Nishikurosawa Formation, which contains oil and gas, consists of basaltic lava, mudstone and acidic pyroclastic rock. Onnagawa and Funakawa Formations are comprised of mudstone, and these are considered to be the source rocks. The hydrocarbons generated in these formations migrated eastward through Kitayuri thrust fault (see Fig. 9c). The study area is characterized by several N–S-trending folds and faults. Due to thrust faulting, several anticlinal structures are formed. These anticlines may be seen in the cross section of Line G2 (Fig. 9b), which indeed corresponds to the MT profile Line B. The MT survey in this area, which aims at delineating these structural features, was conducted along three traverses, Line A, Line B and Line C (Fig. 9a), and these are covered by 27, 25 and 23 MT

Fig. 8 Sediment thickness map of western part of Narmada–Son lineament region from integrated modeling studies (Harinarayana et al. 2003; Singh and Arora 2008)
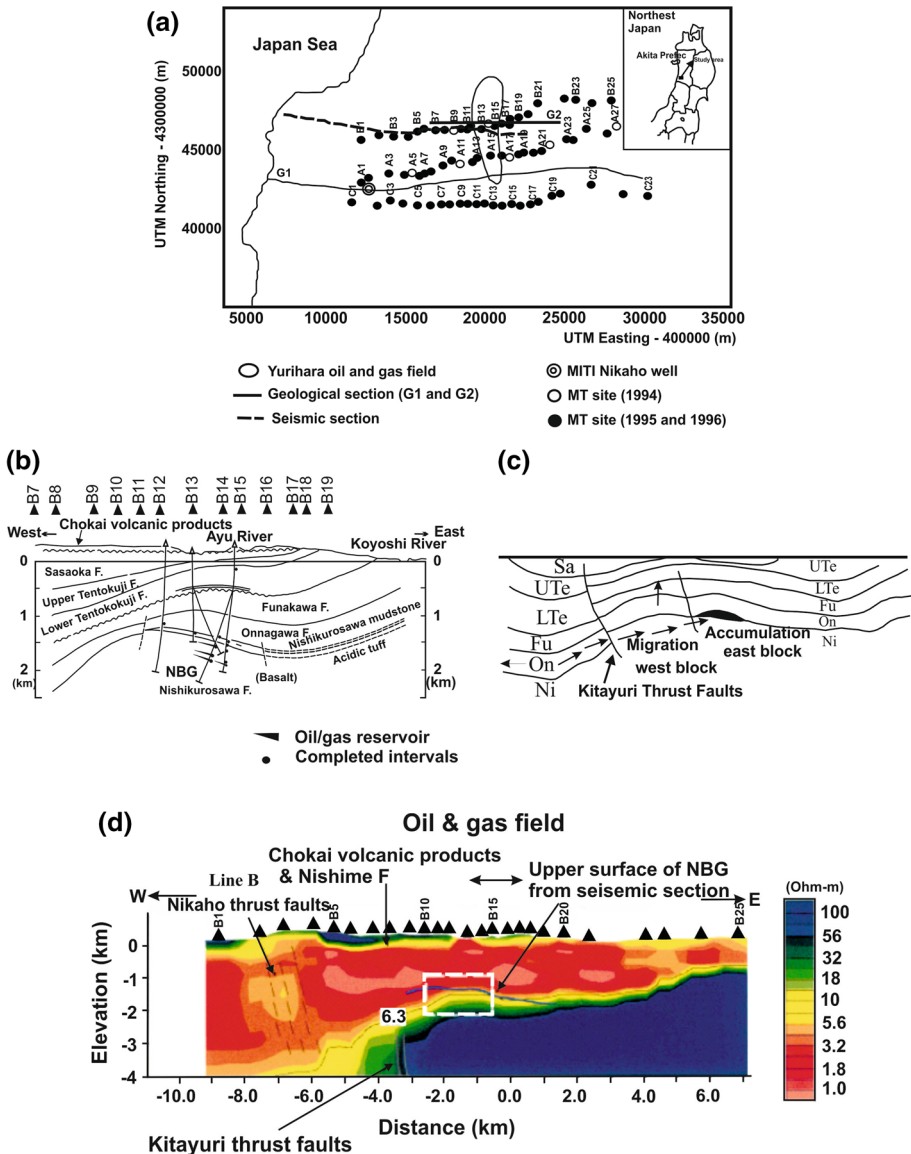
Fig. 9 **a** The location map of the MT sites across Yurihara oil and gas field (redrawn from Mitsuhata et al. 1999). A total of 75 MT stations were occupied along these three profiles. The Yurihara oil and gas field is located in the central part of the survey profiles, **b** A geological section along line G2 (after Ichinoseki 1984). MT site locations on line B are shown. **c** Migration and accumulation model of hydrocarbons during Sasaoka Age in the Yurihara oil and gas field (modified after Waseda and Omokawa 1990). **d** Two-dimensional geoelectric section along line B is shown

sites, respectively. For the 2D analysis of the MT data, smooth-constrained 2D inversion codes developed by Uchida and Ogawa (1993) and Uchida (1993) are used. Thirty-three frequencies in the range of 160–0.003 Hz are used for the 2D inversion. The MT section from 2D inversion of data along the line B in the Yurihara oil field has brought out an

upward folded resistive feature lying under a thick conducting layer (Fig. 9d). The uplift, which can be seen on the eastern side of the section spatially, correlates with the known reservoir.

2.4 Eastern Siberia, Russia

Several regional level MT surveys were carried out in Russia to image Earth's crust, including the shallow sedimentary cover (Fig. 10). The MT data sets obtained from the regional level MT surveys were also utilized for probing the shallow sedimentary cover as well, for hydrocarbon exploration. From these studies focusing on the sedimentary cover, several structural features such as folds, reef structures and salt domes. relevant to hydrocarbon exploration were inferred. The effectiveness of integration of MT and seismic results is illustrated below through an example from Tunguska basin in eastern Siberia.

A seismic survey was carried out along the 3-SB profile, and a reef massif is imaged (Fig. 10). An MT study was carried out (Berdichevsky et al. 2015) to examine the electrical structure and evaluate the resistivity characteristics of different formations. One-dimensional constrained inversion of MT data was carried out for this purpose. The available well log data were also used in correlating with the result of MT study.

The geology of the study area consists of the Proterozoic and Phanerozoic sediments overlying the Archean basement. The Proterozoic portion consists of Lower to Upper Riphean (1400–800 Ma) and Vendian (650–543 Ma). Phanerozoic consists of Paleozoic and Mesozoic sediments. The sections on both sides of the reef (Fig. 10) are mainly halogenous carbonates, and these are believed to be the source rock, and toward the north of the reef, the thickness of these formations decreases. The main objective of the study is to image the reef system and the underlying Vendian terrigenous sediments, these being the main targets for hydrocarbon exploration. Reef barrier is a type of geological structure where petroleum can be trapped. The reef structure is found to lie in the Upper Cambrian strata above the Vendian.
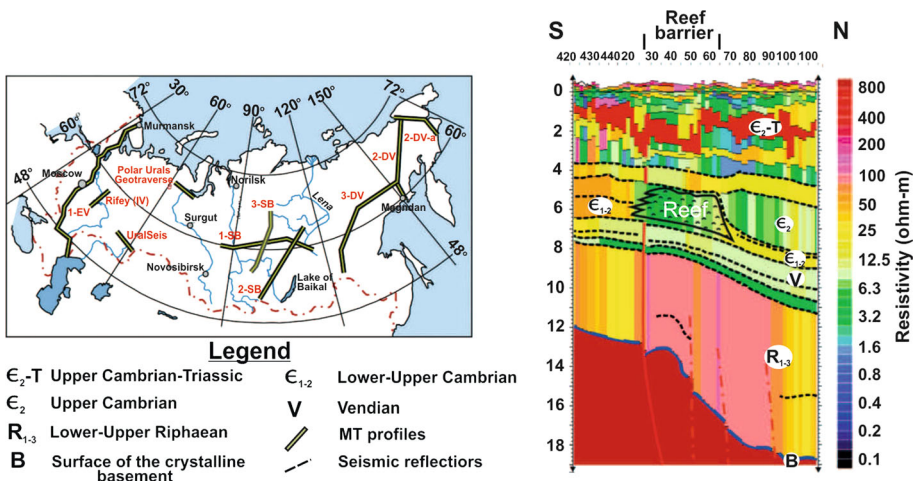

Fig. 10 Location of MT transacts in Russia (left) and seismic constrained MT section of reef barriers in eastern Siberia (right). The MT model brought out the lateral conductivity variations of each formation (including the hydrocarbon prospective formation) imaged by seismic and confirm the presence of reef structure which is characterized by relatively conductive feature

The MT data along the 3-SB profile shown in Fig. 10 are used for illustrating the role of MT application in this example. The data from 13 stations along a 50-km-long stretch are selected. One-dimensional inversion of the data is used to obtain the resistivity of different layers, and the results correlate well with the well log data. It is interesting that MT results brought out a characteristic conductive nature of the reef with a resistivity of about 3 Ωm. The results show that the granitic basement, as well as the volcanic trap, shows resistivities of about 800 Ωm. Further, the MT model suggests that on both sides of the reef structure (ε_{1-2}) the medium is moderately resistive (about 60 Ωm), while the reef itself is highly conductive. From these, it is interpreted that the reef is porous and the hydrocarbons are trapped in it as resistive sections are present on both sides.

2.5 Pre-Caspian Depression, Russia

The exploration for oil in the Altatino–Nikolskaya area at the northern edge of the Pre-Caspian depression, Saratov region, Russia, is an interesting case where the MT application was found to be highly effective (see Berdichevsky et al. 2015). The geological setting of the Pre-Caspian depression is complex due to the presence of several salt domes. The sedimentary cover in the area consists of three layers, viz. conducting suprasalt Mesozoic sediments, highly resistive Kungurian salts and resistive sub-salt horizon. MT is highly effective in imaging such subsalt structures even at depths of more than 10 km, and it is shown to be very efficient in subsalt mapping even in the presence of highly conducting suprasalt rocks.

An MT study was carried out in this region in 2004 for identification of the target. Station spacing was 1–5 km. Since modeling methodology is to be chosen based on the expected subsurface structural configuration at different depth levels, in the present case, 1D modeling was considered to be enough to image the Mesozoic suprasalt sedimentary cover, as this is characterized by a horizontal layered structure. However, the deeper structure is not 1D. MT results from 2D inversion show that the resistivity of the Mesozoic rocks in the area varies over a range of 1–30 Ωm, with the higher values occurring at deeper levels. The thickness of suprasalt sedimentary cover varies from 100 to 300 m over the salt domes, and it becomes much thicker up to 4 km in other regions (Fig. 11).
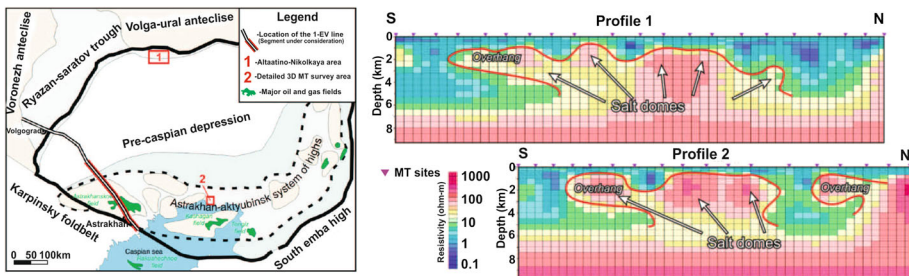

Fig. 11 Left: Location of the magnetotelluric survey and the tectonic map of Pre-Caspian depression. Right: Two-dimensional resistivity representation along two profiles in Altatino-Nikolskaya region in which salt domes are imaged. Note that the resistive portion in the model is shown as red color, and the conductive portion of the model is shown as blue color

2.6 Qaidam Basin, China

The Qaidam Basin, a hydrocarbon producing basin, is located in west-central China on the northern flanks of the Qinghai–Tibet Altiplano (Fig. 12). The source rock is the shallow lacustrine, dark mudstone of the Qigequan Formation of the Quaternary and the Shizigou Formation of the upper Tertiary. The source rock has a good generation potential, leading to large biogenic gas reservoirs in the area. Three-dimensional continuous electromagnetic profile (CEMP), a new MT method proposed by He et al. (2010a, b) to locate new gas reservoirs, was used for the investigation of this target area. The CEMP method is an offshoot of MT method in which continuous electric field is acquired, followed by 3D inversion. In addition to resistivity anomalies, hydrocarbon-bearing formations are known to display anomalous polarization conditions also in some areas (for, e.g., see Zonge et al. 1972; Davydycheva et al. 2006; Chen et al. 2006; Cao et al. 2006; Davidenko et al. 2008). Using both resistivity (R) and induced polarization (IP) anomalies, He et al. (2007) defined a new anomaly, IPR (IPR = IP × R). In the present example, the resistivity and IP anomalies derived from high-precision CEMP data are used to identify potential hydrocarbon zones based on the IPR values (He et al. 2010a, b).

CEMP studies were carried out along the test line (marked as a red dotted line in Fig. 12), which passes through the known gas field (SB-1) and a dry well (KN2). Figure 13a, b shows the apparent resistivity and phase pseudosections along this line. The
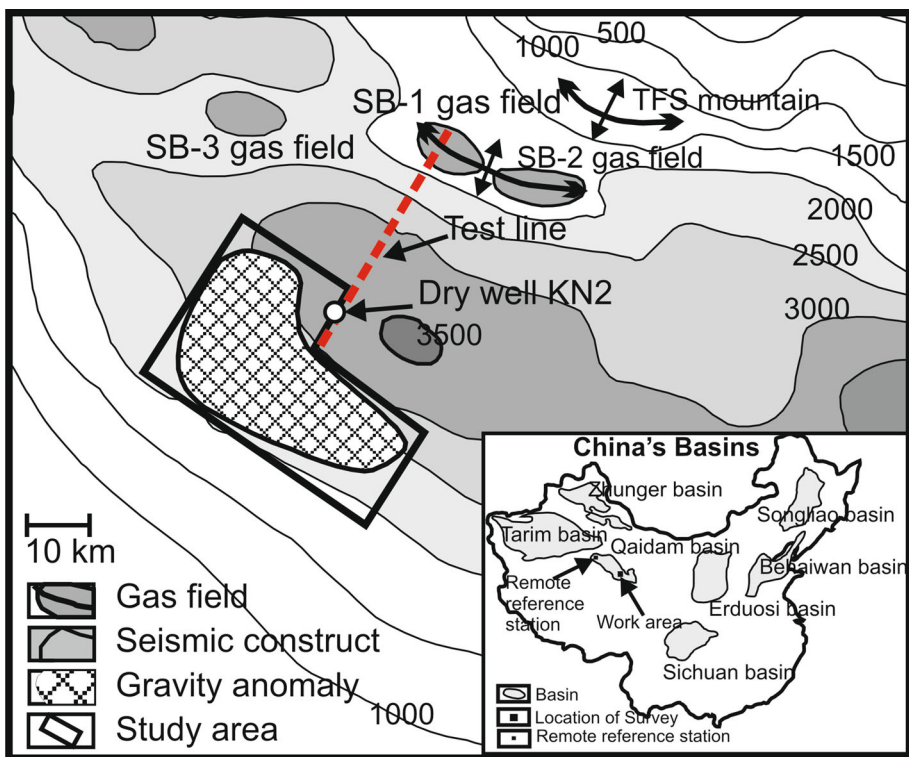
Fig. 12 Study area and the location of Qaidam Basin, China (redrawn from He et al. 2010b). The test line is marked as a red color for which both CEMP and IP data were obtained

sections indicate anomalous high resistivity and low-phase zones beneath the gas field as compared to the dry well. Two-dimensional inversion result of the CEMP data is presented in Fig. 13d, which indicates a high resistive zone at 1000–1500 m depth. It matches well with the gas field. Figure 13c shows the polarizability section along the same line obtained from 2D inversion of IP data. It seems that the polarizability also shows higher values at the SB-1 gas field. Considering the IPR anomaly, it becomes maximum when both resistivity and IP parameters are high, and according to the IPR theory, the anomalous zone with IPR maximum can be considered as a potential reservoir, and in the present case, it is validated from the spatial correlation of the IPR anomalous zone with the known gas field (SB-1).
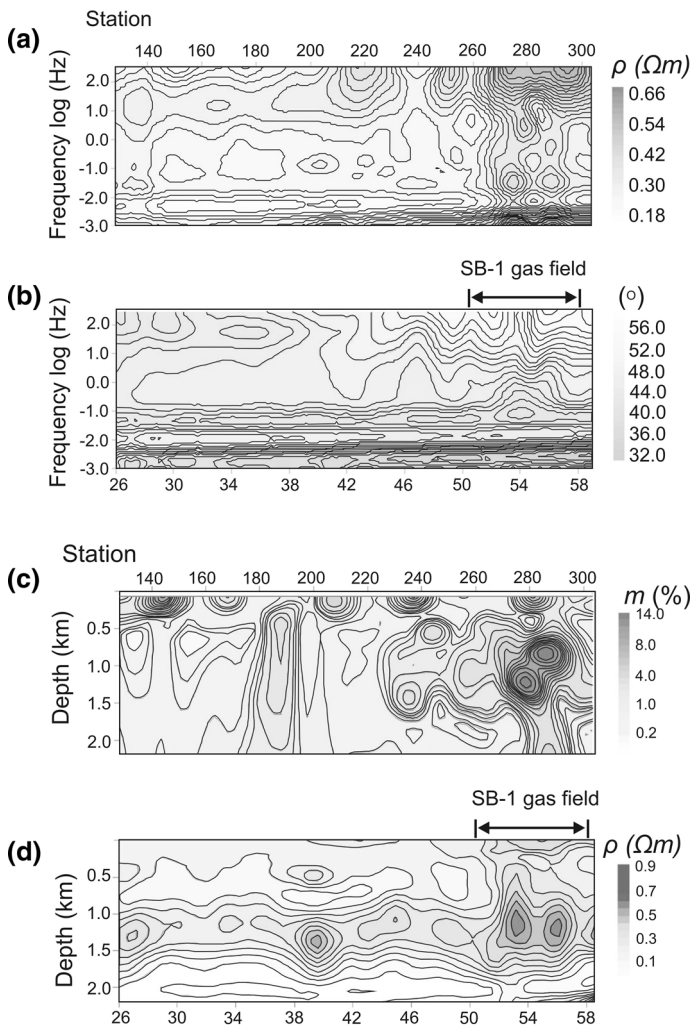
Fig. 13 a Apparent resistivity and **b** phase pseudosection along the test profile. **c** Two-dimensional resistivity model and **d** two-dimensional polarizability result from the test profile (redrawn from He et al. 2010b). It may be seen that the resistivity and polarizability show higher values corresponding to SB-1 gas field

3 Geothermal Studies

3.1 Introduction

A geothermal system basically consists of three elements, viz. a heat source, a reservoir and fluid, which is the carrier that absorbs and transfers the heat. A magmatic intrusion (> 600 °C) at shallow depths (5–10 km) could be a heat source; otherwise, as in a low-temperature system, the source could be the naturally increasing temperature of the Earth with depth which can heat the percolating fluid which can serve as a reservoir. The fluids in geothermal systems are in general meteoric water, and they could be either in the liquid or in vapor phase depending on the temperature and pressure conditions in the reservoir. These geothermal fluids transport heat (thermal energy) from the deep hot rocks to the surface. Figure 14 shows a model representing an idealized geothermal system.

The geothermal systems are classified based on the enthalpy of the geothermal fluids. The geothermal resources are classified as low-, medium- and high-enthalpy resources, according to the energy content of the fluids and their potential forms of utilization. Table 1 presents the different classifications of geothermal resources proposed.

3.2 Geophysical Studies for Geothermal Investigations

Among the geophysical studies deployed for investigation of a geothermal system, EM technique, particularly magnetotellurics (MT), is known to be highly effective since the subsurface electrical conductivity is known to be a very important parameter characterizing a geothermal setting in a target area. This is because the geothermal systems, in general, are associated with structures such as faults, fractures and shear zones which act as
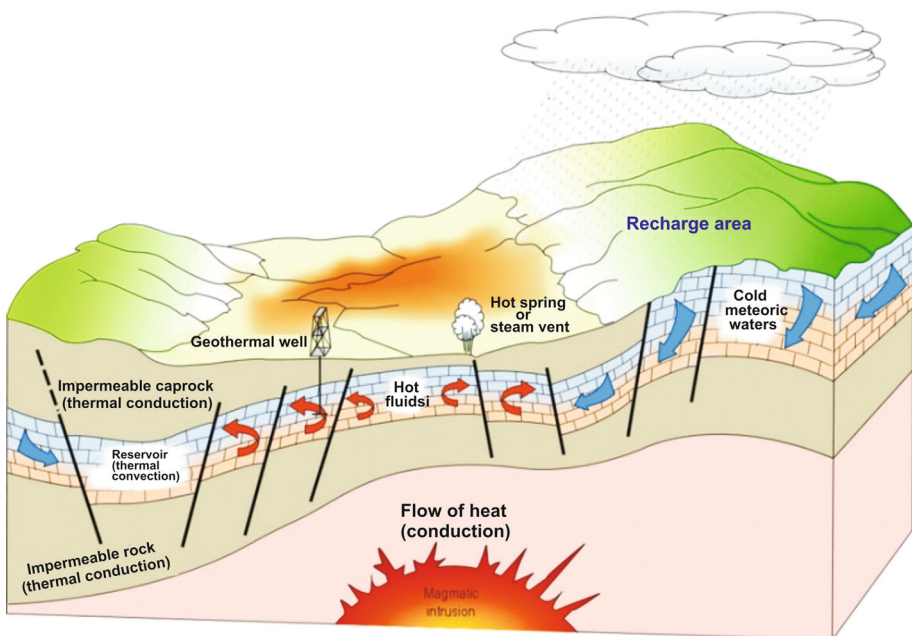
Fig. 14 A representative diagram of an ideal geothermal system (taken from www.geothermal-energy.org)

Table 1 Classification of geothermal source. Temperature is in °C

Source	Muffler and Cataldi (1978)	Hochstein (1990)	Benderitter and Cormy (1990)	Nicholson (1993)	Axelsson and Gunnlaugsson (2000)
Low-enthalpy resources	< 90	< 125	< 100	<= 150	<= 190
Intermediate-enthalpy resources	90–150	125–225	100–200	–	–
High-enthalpy resources	> 150	> 225	> 200	> 150	> 190

conduits for the circulation of geothermal fluids in the rock matrix of the system and very often these fluids, because of dissolved salts, act as electrically conducting electrolytes, thus imparting a conductive nature to the structural features. The temperature of the system further modulates the electrical conductivity of the assembly. Thus, the geothermal system including fluids and rock matrix in general presents itself as an electrically anomalous conductive target and the EM methods, MT in particular, become the favorite tool to detect and image such significantly anomalous conductive zones over a range of depths in a given region of geothermal significance. Several researchers have applied EM techniques to map the subsurface conditions of the geothermal regions of both high- and low-enthalpy target areas in different countries in Asia, for example Japan (Yamane et al. 2000; Mustopa et al. 2002; Uchida 2003, 2005; Ushijima et al. 2005; Spichak 2005; Nurhasan et al. 2006; Umeda et al. 2006; Asamori et al. 2010; Uchida et al. 2011; Aizawa et al. 2014; Ogawa et al. 2014; Seki et al. 2015), Korea (Song et al. 2003; Lee et al. 2004, 2007, 2010, 2015; Uchida et al. 2005), Taiwan (Chang et al. 2014; Komori et al. 2014; Chiang et al. 2015), Philipines (Banos 1997; Reyes 1999; Layugan et al. 2005; Banos 2012; Austria et al. 2015), Indonesia (Maryanto et al. 1992; Raharjo et al. 2010; Sumintadireja et al. 2011; Niasari et al. 2012; Parnadi et al. 2014; Zarkasyi et al. 2015), Vietnam (Tuyen et al. 2015), Thailand (Amatyakul et al. 2015, 2016), China (Bai et al. 2001; Wu et al. 2012; Zhang et al. 2015), Russia (Zakharova et al. 2007), India (Sinharay et al. 2001; Bhattacharya et al. 2003; Harinarayana et al. 2004; Sinharay et al. 2010; Rao et al. 2014; Patro et al. 2015b; Sircar et al. 2015), Iran (Oskooi and Darijani 2013; Oskooi et al. 2016), Saudi Arabia (Lashin and Arifi 2014; Lashin et al. 2015), Turkey (Rosario et al. 2005; Kaya and Basokur 2010; Rosario and Oanes 2010; Ayka et al. 2015; Leeuwen et al. 2015), and for other parts of the world, see the review papers by Berktold 1983; Meju 2002; Spichak and Manzella 2009; Munoz 2014).

Meju (2002) discussed the geological settings of the volcanic and non-volcanic geothermal system and the different ground electrical and electromagnetic methods being used for geothermal exploration along with case studies. Berktold (1983) discussed the dependency of electrical conductivity of the fluid and rocks on several physical parameters in the geothermal region followed by a discussion on different geothermal systems and proposed an idealized model of a hyper-thermal field. He later discussed different electrical and electromagnetic techniques and their application in geothermal exploration with relevant case studies. Munoz (2014) followed a site-oriented approach in presenting the results of the application of electrical and electromagnetic methods. He has also provided some case studies based on high-enthalpy and low-enthalpy systems. He has also

emphasized the shortcomings in the modeling and interpretation of EM data for geothermal exploration.

As may be seen from the above studies, to interpret the observed MT responses for a given area it will be advantageous to have a conceptual model of the geothermal target and its response. As mentioned before, the geothermal systems may be broadly divided into two divisions depending on the nature of thermal source: (1) magmatic and (2) non-magmatic.

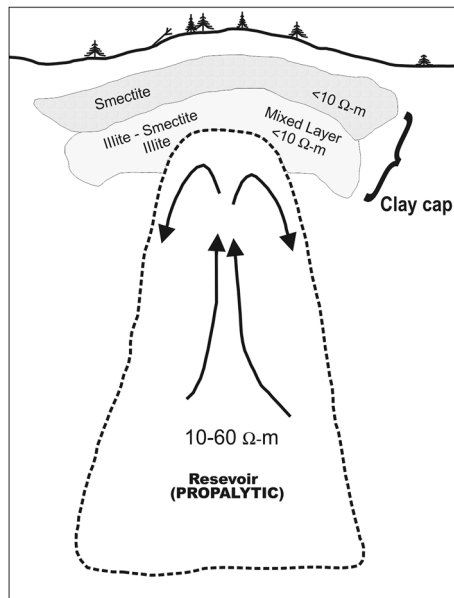### 3.3 Magmatic Source (High-Enthalpy Systems)

While the enhancement of conductivity of subsurface target region is a common feature for both the systems, in the case of high-enthalpy systems supported by magmatic source, geothermal processes often lead to generation of extensive clay mineral (smectite, illite) alterations, which under favorable conditions can form a well-defined high conductive clay cap over the geothermal reservoir (Wright et al. 1985).

Thus, the electrical model for such a situation may be characterized by a high conductive top layer ($< 10 \, \Omega$m) representing the clay cap, underlain by a relatively less conductive body representing the reservoir source. Figure 15 shows such a conceptual model, which is typical of high-temperature magmatic geothermal fields.

3.4 Non-magmatic Source (Low Enthalpy)

For non-magmatic geothermal systems, the main constituents to be identified are the deeper aquifers that can act as reservoirs and fluid pathways. In the case of low-enthalpy

Fig. 15 Conceptual model of a geothermal system (redrawn from Pellerin et al. 1996)

geothermal system (non-magmatic source), however, the electrical responses vary over a wide range. The electrical imaging of low-enthalpy geothermal targets primarily aims at locating the deeper hot water aquifer zones, representing the reservoir systems, as also mapping the fluid path ways wherever possible, but the non-magmatic geothermal systems exhibit a wide range of variation in structural geometry, lithology and composition. In some cases, the natural permeability of reservoirs is enhanced through additional stimulations of fluid path ways (enhanced geothermal systems). It becomes difficult to build a generalized conceptual model in the case of low-enthalpy target areas because the nature of conductivity anomalies associated with such complex geometries can vary over a wide range. Several low-enthalpy geothermal systems have been studied in Southeast Asia, located in different geological and tectonic environments such as those in Philippines (Mabini, Rosario and Oanes 2010), Korea (Pohang, Uchida et al. 2005; Lee et al. 2007) and India (Harinarayana et al. 2004, 2005a, b, 2008; Sarma et al. 1983; Sinharay et al. 2010; Patro et al. 2015b).

To illustrate the above features in terms of geophysical responses, we present here a few case studies of geothermal investigations carried out over different geological and structural environments in Asia.

## 4 Some Case Studies of MT Application for Geothermal Studies in Asia

4.1 Hailin Geothermal Anomaly, Mudanijang, NE China

Magnetotelluric studies were conducted along three parallel profiles traversing across the geothermal target bodies in Hailin, Mudanjiang area, in the northeast China (Zhang et al. 2015). The MT data were processed using the mutual reference method. The geoelectric image derived from 2D inversion (Fig. 16) shows that a highly resistive granite basement is covered with conductive sediment layers and that a relatively low resistive anomalous structure with a resistivity of nearly 100–600 Ωm is embedded in the high resistive background. The anomalous structure has a narrow top and a wide bottom resembling a cone-shaped body (Fig. 16). The shape and electrical character of the structure indicate favorable storage conditions and space for hot subsurface water.

Faulting and magma intrusions often result in fracturing of the basement rock, and when the fractures are filled with hot water, they reflect in the electrical imaging as conductive features. Occurrences of high temperatures are confirmed by an exploratory well. The presence of cap rock, basement and major faults are necessary to generate favorable conditions for the development of a geothermal reservoir (Wright et al. 1985; Pellerin et al. 1996). In this case, the structure below Hailin is not consistent with the conventional model as proposed by Wright et al. (1985) and Pellerin et al. (1996). The fractured zones of the faults facilitate the migration and supplementation of heat and groundwater (Sui et al. 2011). The sedimentary formations with large thickness and poor thermal conductivity prevent subsurface heat from diffusing and act as a cap rock.

4.2 Lahendong and Kamojang Geothermal System, Indonesia

Lahendong and Kamojang are two important geothermal fields located in Indonesia with significant power production potential, with current capacities of 40 and 200 Mw. Three-dimensional MT studies were conducted in both these fields to understand the subsurface
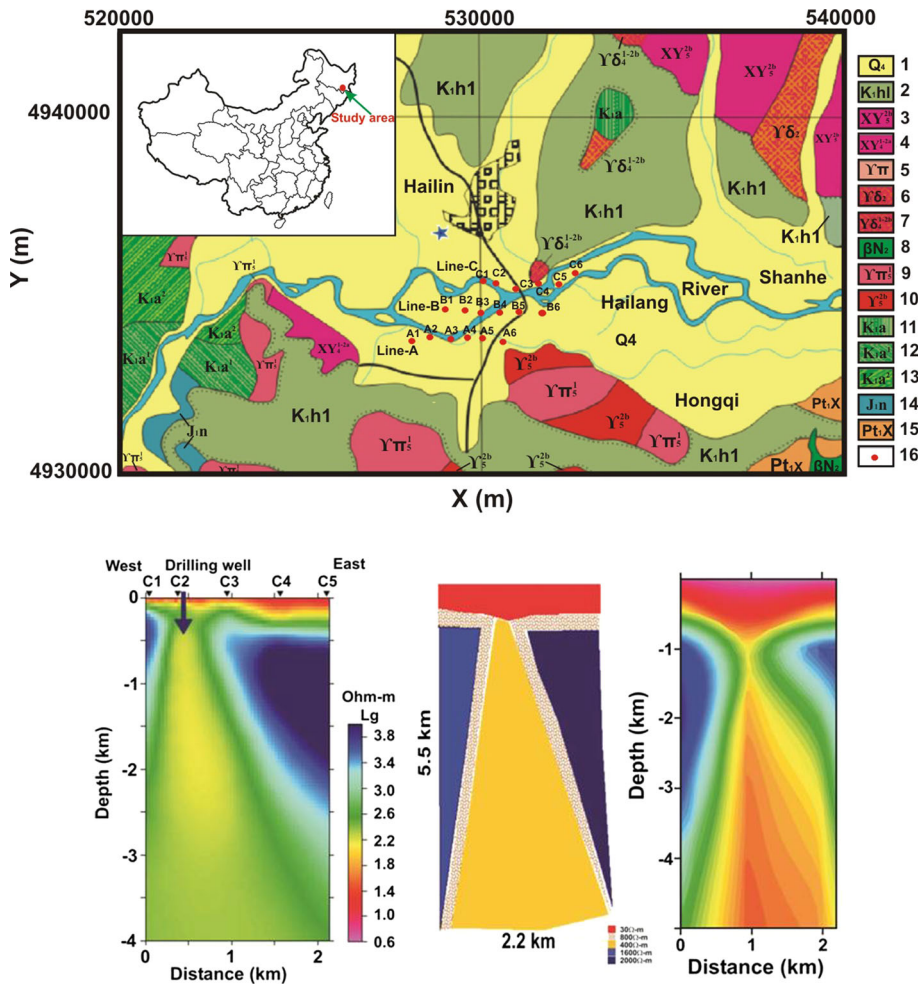
Fig. 16 Top: Regional geological map of the MT survey area. Bottom: 2D electrical model along C profile (left). Dark blue arrow shows the location of exploratory well (reaching to a depth of 655 m) drilled near site C2. A 2D synthetic model was prepared taking the structure from the model along C profile to test the robustness of the model (middle), and the joint (TE and TM) inversion of the synthetic data presented to the right (modified after Zhang et al. 2015) shows that the inversion can recover the synthetic model

electrical structure related to the nature and configuration of the geothermal reservoirs (Raharjo et al. 2010).

The Lahendong field (see Fig. 17 for location) is known to be characterized by a liquid-dominated reservoir in the northern part and a two-phase reservoir in the southern part. The MT inversion results in the case of Lahendong geothermal field brought out a domal structure with resistivities in the range 20–60 Ωm capped by a conductor (< 10 Ωm) as depicted in Fig. 18a, b, which shows the horizontal sections for two different levels, taken from the 3D MT model obtained for the area. The structure resembles a propylitic reservoir encapsulated by geothermal clay caps. It may be seen the location of the major well LHD-23, drilled in the area falls in the area corresponding to the central block of the dome where

the propylitic region, showing an areal extent of 3×4 km^2 lies at a depth of 1.5 km (Fig. 18a, b).

Kamojang, on the other hand, is a vapor-dominated system and is hosted in a caldera surrounded by volcanic ranges. The MT inversion results (Raharjo et al. 2010) brought out a highly useful electrical image of the target area. The 3D MT model (Fig. 18c, d) indeed shows an electrical conductor emerging from the fumarolic area, located in the north-eastern corner of the caldera, and the feature extends downwards into the caldera. As it goes further down to a depth of about a kilometer, the conductor becomes pervasive as it comes into the proximity of the propylitic zone. Further down, the 3D electrical model shows a well-defined subsurface U-shaped west-facing resistive ridge-like feature, around a depth of 1.5 km, which is interpreted to represent the vapor-dominated zone and is considered to be the source of the vapor being fed to the power plant in the area. This U-shaped propylitic ridge is considered to be closely linked to the Kamojang caldera structure. Further westwards, this feature opens up and tends to become gradually conductive toward the west and it is this western part of the zone that corresponds to the observed two-phase characteristics of the source region.

4.3 Hydrothermal System Beneath the Jigokudani Valley, Tateyama Volcano, Japan

Jigokudani valley, hydrothermal system an important geothermal source, has been investigated using an audio-frequency magnetotelluric (AMT) survey (Seki et al. 2015). This survey has been conducted to understand the subsurface electrical structure and study its relationship to the geothermal activity in the Jigokudani valley. Two-dimensional inversion of AMT data collected at eight locations across the valley helped to provide evidence for the presence of an interesting structural scenario (Fig. 19) characterized by a shallow conductive layers (C1 and C2) in the area up to 500 m depth which in turn rests on a resistive layer (R1). The resistive layer is cut across by a moderately conductive narrow linear zone (C3) that extends upwards sub-vertically toward the shallow conductive region.

The top conductive layer itself is comprised of an upper relatively lower conductive part (C1) inferred to represent the lacustrine sediments of an extinct crater, and the lower section (C2) corresponds to the segment holding thermal fluids as well as vapor. The upper clayey sediment zone (C1) with its low permeability acts as a clay cap that facilitates the
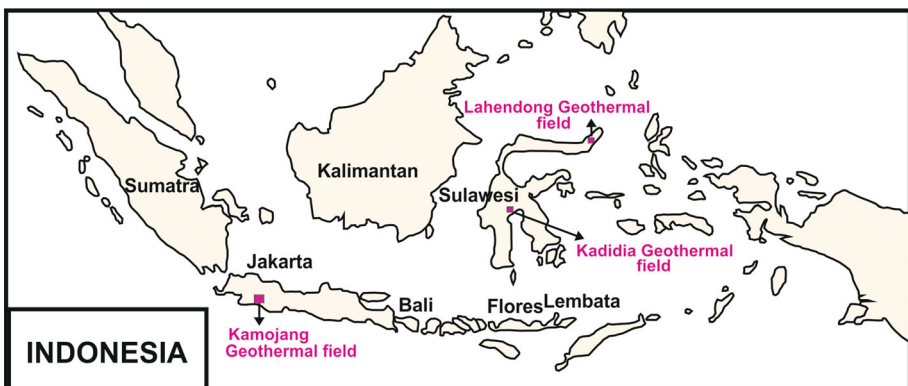
Fig. 17 Location of Kamojang, Kadidia and Lahendong geothermal fields in Indonesia
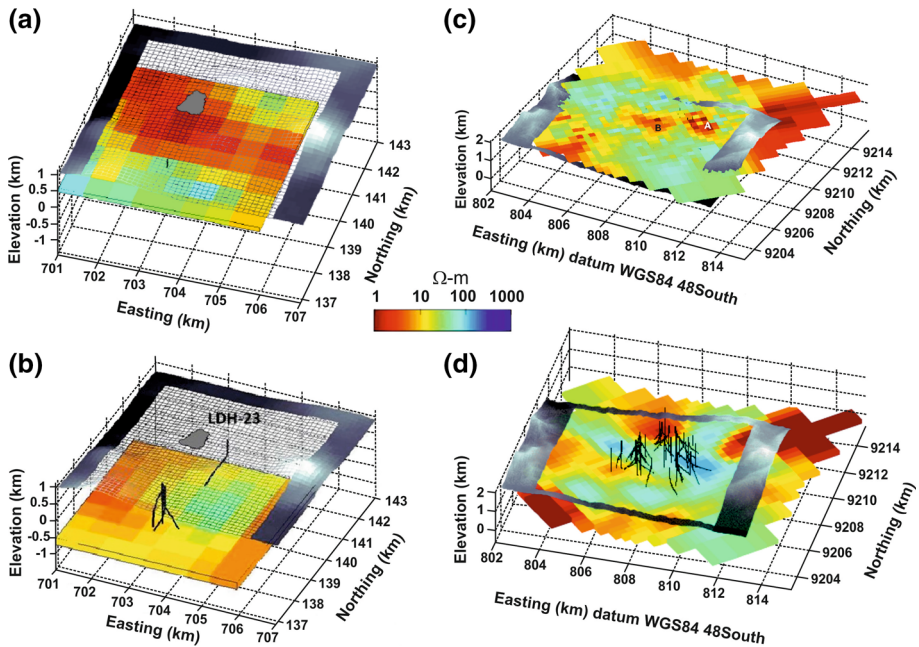
Fig. 18 **a**, **b** Subsurface electrical image of Lahendong, at a depth of 475–600 masl and −700 to −500 masl overlain by a topographic mesh. LDH 23 is the well track. **a**, **b** Represents horizontal electrical cross sections at two different levels cutting across the domal structure identified from the MT studies. **c**, **d** Resistivity images of the Kamojang geothermal region (60 m thin slice situated at 1400–1460 masl and 200 m slice situated from − 0.075 to 125 masl) (modified after Raharjo et al. 2010). West-facing U-shaped resistive zone representing vapor-dominated zone may be seen in the deeper section (**d**)
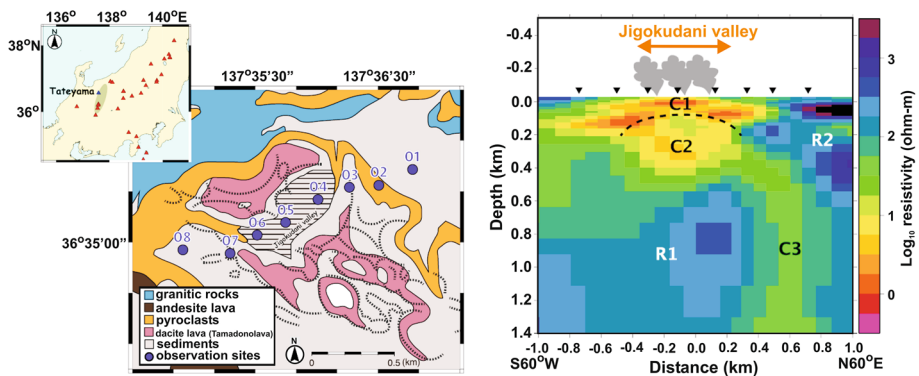
Fig. 19 (Left) Simplified geological map of Jigokudani Valley, Japan. The hatched region shows the Jigokudoni valley, and the dotted lines represent the traces of hydrothermal eruption craters. Inset map shows central Japan, where the red triangles show the locations of active volcanoes. (Right) 2D resistivity model across the Jigokudoni valley. Inverted triangles are the locations of AMT sites. The gray smoke cartoon represents the fumarolic zone. C1–C3 and R1, R2 are discussed in the text

accumulation of fluids and vapor underneath this cap structure. While the high resistive zones (R1 and R2) correspond to the granite rock matrix, the moderately conductive narrow linear zone that cuts across the resistive granites and gets connected to the top conductive zone is interpreted to serve as a conduit for transmission of high-temperature volcanic gases to shallower levels (Fig. 19). Seki et al. (2016) carried out three-dimensional modeling using more sites, and the results are consistent with the resistivity structure shown in Fig. 19.

4.4 Yanaizu–Nishiyama Geothermal Field, Northeastern Japan

The Yanaizu–Nishiyama geothermal field in northeastern Japan is another typical example of a high-enthalpy geothermal system in Asia. In this region, already a 65-MWe geothermal power plant has been operational since 1995. However, after several years of operation, the capacity dropped to 50 MWe. This has necessitated further investigations, and hence, a 3D magnetotelluric study of the region was carried out during 2010 (Uchida et al. 2011). In addition to the 30 stations occupied during 2010, earlier MT data acquired by Geological Survey of Japan during 2000 and 2001 were also used for modeling and interpretation. Despite the problems of external noise, the electrical image derived from 3D inversion of MT data (Fig. 20) is found to be quite useful. The 3D model has delineated shallow low resistive zones corresponding to three major known faults in the area. Besides these, it has brought out the upper and lower boundaries of the conductive clay cap layer and also mapped the feed zones identified in production boreholes which seems to be located underneath the high conductive cap layer (red part in Fig. 20).

4.5 Pohang EGS Pilot Site, Korea

Several geological and geophysical exploration studies, including seismic, gravity, magnetic and magnetotellurics (MT), were conducted in the Pohang geothermal site since 2003
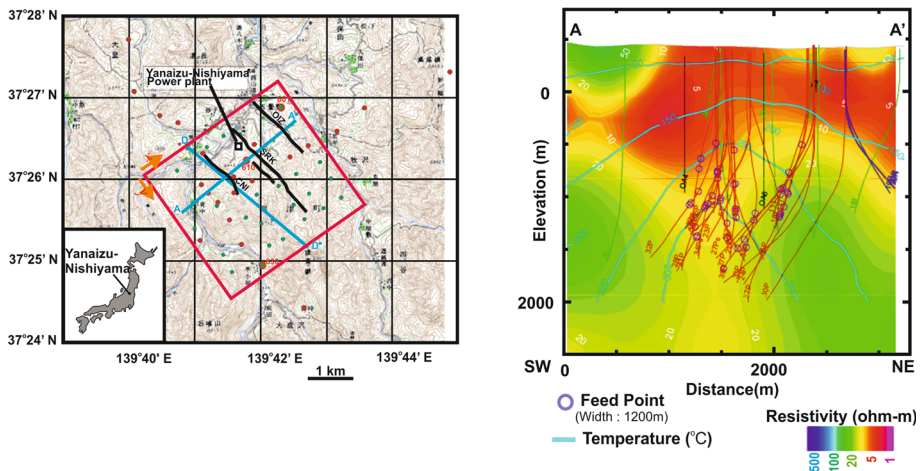

Fig. 20 Location map of the MT station at Yanaizu–Nishiyama geothermal field. Three-dimensional resistivity model along profile AA′ with projected borehole trajectories. The temperature contour is also superimposed on the model. The temperature zone is consistent with the resistivities corresponding to the reservoir zone (modified after Uchida et al. 2011)

(Song et al. 2003; Lee et al. 2004; Uchida et al. 2005; Lee et al. 2007, 2015). For exploitation of geothermal resources, five deep boreholes were also drilled. Later in 2010, another deep well, PX-1 was drilled which reached a depth of 4127 m. The drilling results show a layered structure with a surface layer corresponding to Quaternary alluvium deposits sitting over a thick Tertiary sedimentary layer. Some plutonic intrusions are also identified. The geophysical results suggest in general NNE–SSW running lineament and fracture pattern in the southern part of the Heunghae Basin. It is interesting that potential geothermal reservoirs in Korea are mainly controlled by such fracture zones that generally extend to deeper levels of the crust. The 3D MT modeling results (Lee et al. 2007) for the area brought out a well-defined layered structure with a conductive top layer sitting over a resistive bottom layer (Fig. 21). The shallow conductive layer from the MT model is fairly consistent with the bore well data. The 3D inversion results of MT data indeed point out to a deep extended conductive feature possibly reflecting the intersecting zone of two fractures at the test well BH-2 (Fig. 21). Based on the integration of drill data with geophysical modeling results, a 3D geological model is constructed (Lee et al. 2015).

4.6 Seokmo Island, Korea

Two-dimensional and three-dimensional inversions of MT and AMT data in Seokmo Island, Korea (Lee et al. 2010), helped to identify a well-defined conductivity anomaly at depths of several hundred meters. The conductivity anomaly (Fig. 22) is interpreted to reflect a system of faults/fracture system filled with saline water that extends to at least depths more than 1.5 km. Drilling in this zone indeed has established the presence of a copious amount of thermal water at temperatures of more than 70 °C. The fault/fracture system, hosting geothermal water, is found to be along the boundary between the Cretaceous granites in the north and the Precambrian schists in the south in the Seokmo Island
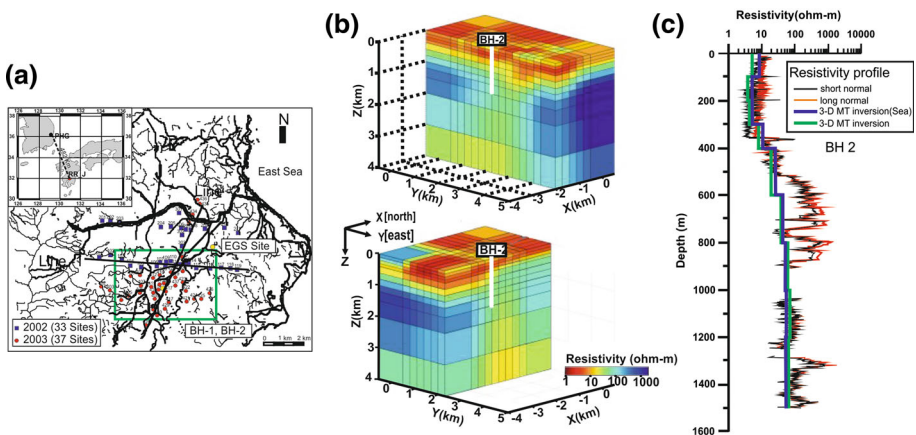

Fig. 21 **a** The study areas with the location of MT stations are shown on the left. Inset figure shows the location of remote station that was operating at Kyushu Island in Japan which is ∼ 480 km away from the study region. **b** Resistivity models derived from 3D inversion of MT data with sea included are presented. The top conducting layer represents the semi-consolidated sediment layer (< 10 Ωm) sitting on a resistive (a few hundred of Ωm) layer. The location of test borehole (BH-2) is overlain on the model. **c** A comparison of resistivity log and the resistivity model from 3D inversion is presented (modified after Lee et al. 2015). Note that the resistive layer was not resolved by 3D inversion which could be due to larger block size adopted in 3D inversion and may be due to the fracture system extending to deeper formations (Lee et al. 2007)

area. The external noise environment has unfortunately set limitations to the use of lower-frequency data to probe deeper levels. However, the model obtained from the available data has been found to be very useful as seen from the drilling results, which showed the presence of significant hot water resources when one of the boreholes (BH2) was extended to deeper levels to reach the conductivity anomaly identified in the 3D MT model (Fig. 22).

4.7 Tawau Geothermal Project, Malaysia

The Tawau geothermal field, Malaysia, associated with the Pleistocene volcanic activity which is related to the extension of the Sulu Archipelago Arc-Trench System into the Semporna Peninsula is an interesting area for MT studies. The geothermal field characterized by steam-heated hot springs and volcanic craters and the presence of chloride springs make it a typical thermal zone connected to an underlying thermal reservoir. The subsurface electrical model generated from inversion of MT data along 15 traverses across the area has demonstrated the consistency of MT results with the typical geothermal model envisaged for a high-enthalpy magmatic source (Daud et al. 2010; Barnett et al. 2015). The top conductive (< 15 Ωm) layer down to a depth of about 1000 m represents the clay cap, while the underlying moderately resistive (20–200 Ωm) layer corresponds to the thermal reservoir. The deeper high resistive dome-shaped basement feature represents the hot rock providing the required thermal energy to the shallower reservoir (Fig. 23). Such a
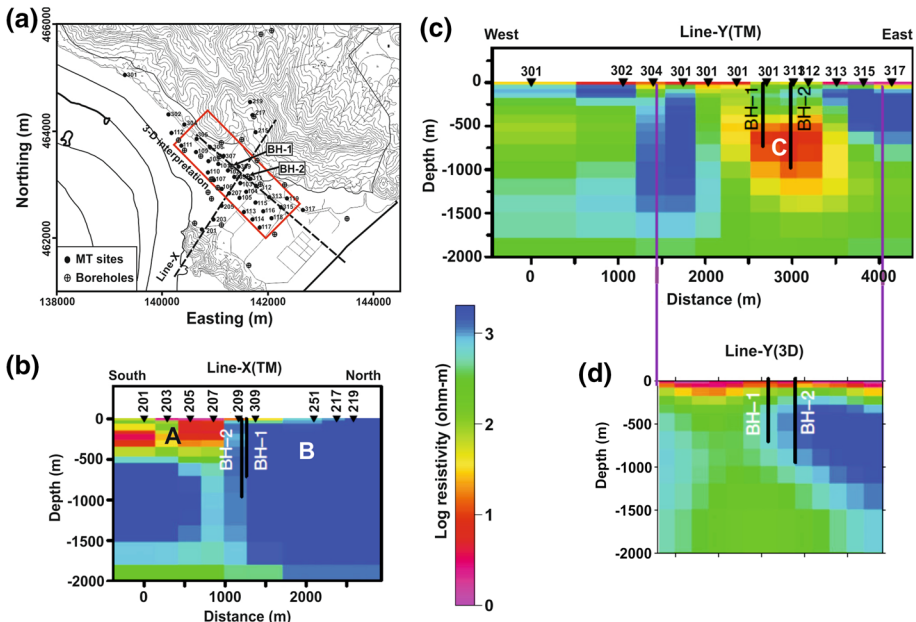
Fig. 22 a Location of MT stations and bore wells. The area covered for 3D inversion is marked as red rectangle, **b** resistivity image along Line-X, A: Shallow fracture system with sea water intrusion B: basement, **c** resistivity image along Line-Y, C: Fracture system that carries geothermal water d) a resistivity section from 3D inversion, note that the boundary coinciding BH-1 is much clearer, which is dipping toward east (modified after Lee et al. 2010). It may also be noted that BH2 is extended to deeper levels, and when it came close to the lower conductor, hydrothermal water appeared in the well

characterization of the subsurface configuration based on the MT models obtained would naturally help to guide the exploration drilling operations for the development of the geothermal field. A 3D conceptual model developed based on the 2D inversion results for this geothermal field is presented in Fig. 24. Additional studies like building 3D inversion models from the data would help to gain further insights into understanding the subsurface configurations of this important geothermal region.

4.8 Saudi Arabian Geothermal Province: First Results from the Al-Lith Area

MT and seismic reflection studies (Fig. 25) were conducted recently (Lashin et al. 2015) in the hot spring area located in the Ain Al-Harrah (surface temperature about 95 °C) and Wadi Markub (surface temperature about 56 °C) areas in western Saudi Arabia. These studies were conducted to image the structural setting related to fault/fracture systems in the country rock, granites. These structural features may be acting as conduits through which the hot water from the reservoir at depth is transported to the surface manifesting as hot springs. The MT data were interpreted using 1D Occam and Bostick inversions. These results show a deeper linear resistive anomaly trending in a near NW–SE direction at a depth of about 2000 m, which is close to that of the Red Sea rift and is consistent with the seismic results. However, a detailed data analysis and applying 2D and 3D modeling approaches to these data sets will bring out the subsurface structure with more relevance.

These results together with the available data on temperature, flow rate and structural setting point out to the necessity of further geophysical studies on a broader scale to image the regional structural setting of the area for evaluating the geothermal potential of the area for initiation of efforts to exploit the same for generation of electricity.

4.9 Geothermal Studies in the Philippines

The Philippines geothermal regions are located in andesitic volcano-sedimentary environments. Since 1995, the Philippine National Oil Company Energy Development
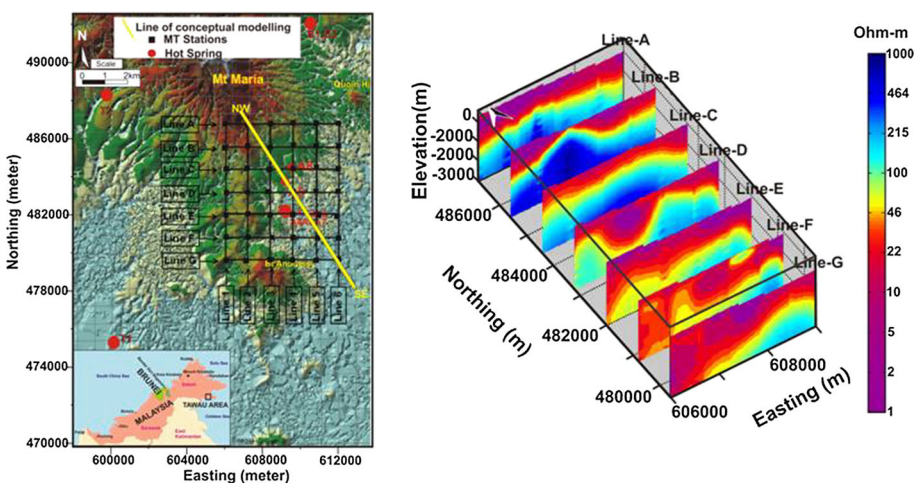
Fig. 23 (Left) Location of Tawau geothermal region and the MT grid. (Right) Two-dimensional inversion models of Line A to Line G
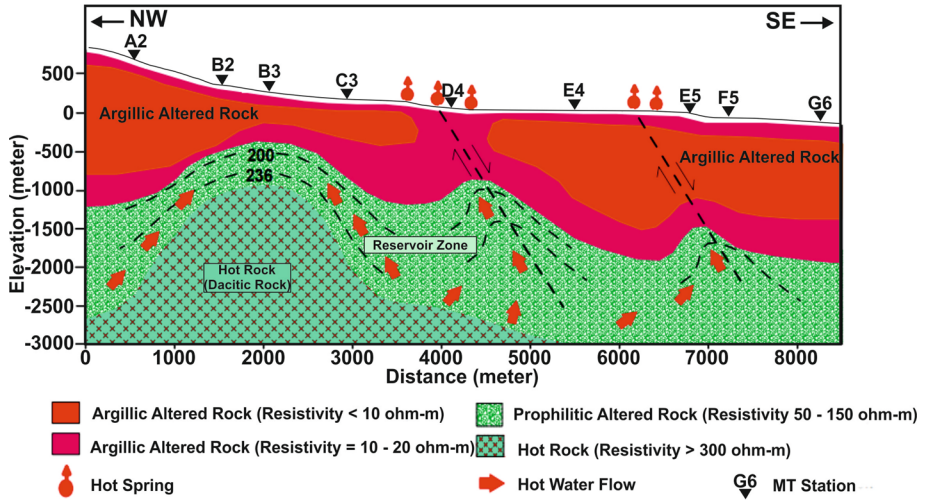
Fig. 24 Conceptual model for Tawau geothermal region (after Daud et al. 2010)
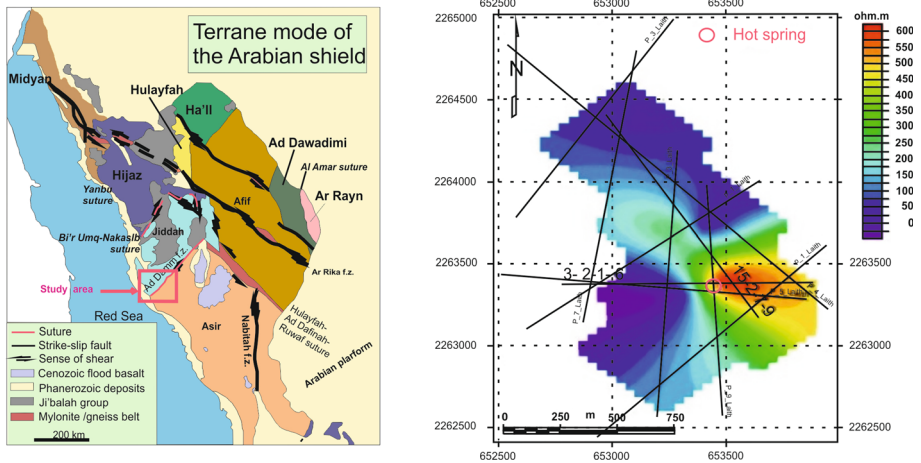

Fig. 25 (Left) Geological map of Arabian shield showing the study area. (Right) Resistivity slice derived from Bostick inversion at a depth of 2000 m. The high resistive region indicates the geothermal anomaly. It may be noted that the color scale is opposite to the conventional color scale used by the MT community

Corporation (PNOC-EDC) acquired MT data at hundreds of locations in various Philippine geothermal areas (Banos 1997; Layugan et al. 2005; Banos 2012; Austria et al. 2015). MT data were recorded for 10 h at each station in the frequency range between 0.00055 Hz and 384 Hz, and remote reference methodology was used where ever necessary.

The electrical model derived from MT data inversion for at least five of the areas in the geothermal belt of Philippines is characterized, in general, by a three-layered structure. The surface layer (thickness < 100–300 m and resistivity of < 100–500 Ωm) corresponds to the young and less altered volcanics. Immediately below the surface layer lies a highly conductive layer with resistivity values of < 10–15 Ωm and of varying thickness. This conductor represents the smectite layer, forming the hydrothermal system's clay cap. The

base of this conductive second layer coincides with the transition from smectite to smectite–illite-dominant argillic alteration. In the central part, the third layer becomes moderately resistive (< 20–100 Ωm) as compared to the surroundings. This relatively resistive segment (> 40–100 Ωm) of the layer block is attributed to a decrease in clay content and presence of less conductive minerals such as illite, chlorite, epidote, biotite and actinolite. Interestingly, this layer corresponds to hottest part of the geothermal system (Fig. 26).

4.10 Puga Geothermal Region, Jammu and Kashmir, India

Puga geothermal province is located in the Himalayan range at an altitude of 4400 m and shows a temperature of 84 °C for its thermal water. This area is located to the south of the Indus suture zone (ISZ), which is the collision boundary between the Indian and Asian plates in the Himalayan orogeny. Results of various geophysical and geochemical studies carried out in this region and its adjoining region (Chumathang) suggest that this is a highly promising area for geothermal exploration and exploitation. During 2001, wide band magnetotelluric soundings were carried out at 35 locations with site spacing of 400 m in the area of known thermal manifestations and at about 1-km spacing in other parts of the Puga geothermal region (Harinarayana et al. 2004, 2006; Abdul Azeez and Harinarayana 2007). Two-dimensional modeling of the data revealed the presence of a high conductive zone toward the west of Sumdo village (Fig. 27). The model brought out a shallow (∼ 400 m) conductor (10–30 Ωm) coinciding with the area of geothermal expressions underlain by a resistive structure followed by another deep conductor (∼ 5 Ωm) at a depth of 2 km. The Kiagor Tso Fault (KTF) acts as a boundary for the geothermal activity and the rest of the region.

4.11 Tatapani Geothermal Region, India

Tatapani hot spring area is located in the vicinity of Narmada–Son lineament zone of India. This region is considered to be one of the significant geothermal areas in the country. Tatapani area exposes Proterozoic rocks comprising of gneisses, granites, schists, phillites of the Chota Nagpur complex in the eastern half and the Gondwana group comprising of
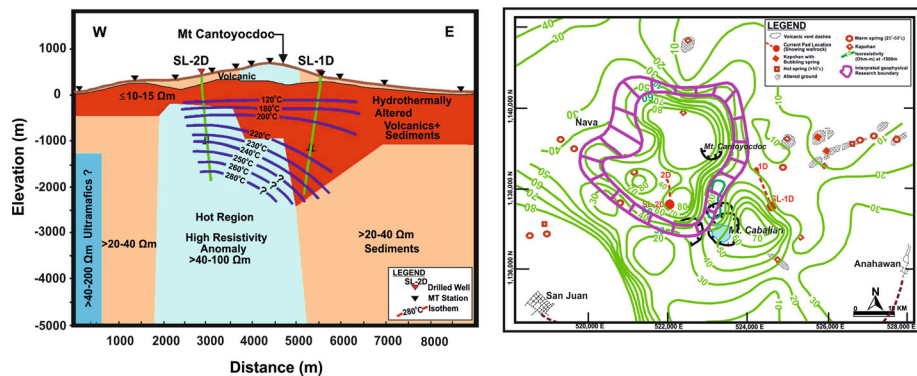

Fig. 26 (Left) Resistivity structure derived from 1D modeling correlates with lithology and temperature at Southern Leyte, Philippines. (Right) Iso-resistivity map at 1500 m elevation and the interpreted geophysical resource boundary of Southern Leyte based on MT

shales, sandstones to the west and northwestern part of the area. The Tatapani fault forms the southern boundary of the coal-bearing Gondwana sediments. A two-dimensional modeling of the MT data set acquired in 1998 was carried out, and the derived model helped to identify a conductive zone (1–10 Ωm) in the depth range of 3–10 km (Hari-narayana et al. 2000a). Later additional MT data were acquired in the Tattapani area during 2015, and a three-dimensional inversion was carried out using the MT data from both 1998 and 2015 field campaigns (Patro et al. 2015b). The modeling results (Fig. 28) brought out the top of the upper crustal conductor which locally rises to ∼ 1.0 km. This high conductive upper crustal feature is inferred to be closely related to the observed anomalous thermal conditions of the area.

4.12 Fang Geothermal Region, Northern Thailand

The Mae Chen thermal system of the Fang geothermal region located in the northern part of Chiang Rai province of Thailand (Fig. 29) is a relatively low-temperature system which does not have any association of volcanism. This hot spring is associated with the EW-trending left lateral strike-slip Mae Chan fault that extends from the northernmost part of Thailand near the Thailand–Myanmar boarder through the Mae Chan region. During 2013, for the first time, to assess the potential of the geothermal reservoir MT survey was carried out with measurements made at thirty-three locations (Amatyakul et al. 2015, 2016). It is
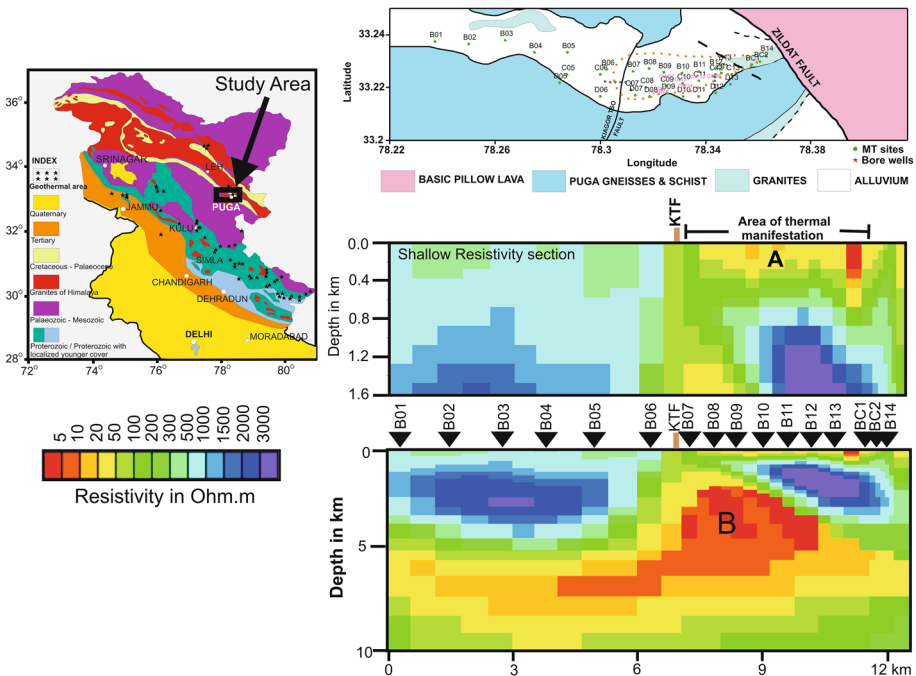

Fig. 27 (Top) Location of MT stations plotted over the geology of the Puga region. The area with thermal manifestation is marked as dotted contour. Shallow (middle) and deep (bottom) two-dimensional resistivity image of the Puga geothermal field derived from inversion of MT data. Thermal manifestation on the surface is shown as A and the deeper conductor B, which is interpreted as a source for thermal anomalies in this area. KTF: Kiagor Tso Fault

believed that the granite batholiths of Mae Chan geothermal system get heated from the deeper granitic batholiths (as a source rock), and the results from the 3D MT modeling (Fig. 30) which show a resistive body (R) at these depths are consistent with such a concept. The Fang sedimentary basin is represented as the low resistive zone (M). Further, at shallow depths, two conductive features C1 and C2 are also mapped which correspond to the sedimentary rocks associated with hot surface fluids from Mae Chen geothermal system.

5 Way Forward

As may be seen from the preceding, the MT serves as a highly valuable and effective geophysical approach in hydrocarbon as well as geothermal exploration strategies applicable to different complex geological and structural scenarios. High-quality MT data obtained over grid patterns in target areas and 3D modeling of such data sets should further enhance its application potential in problem areas. Further, integration of MT results with other CSEM data, which provide valuable subsurface information particularly at relatively shallower levels, as also with well logs and induced polarization would be highly beneficial in arriving at dependable and more detailed subsurface models. Application of other related methods like TFEM, CEMP and induced polarization, wherever necessary, and
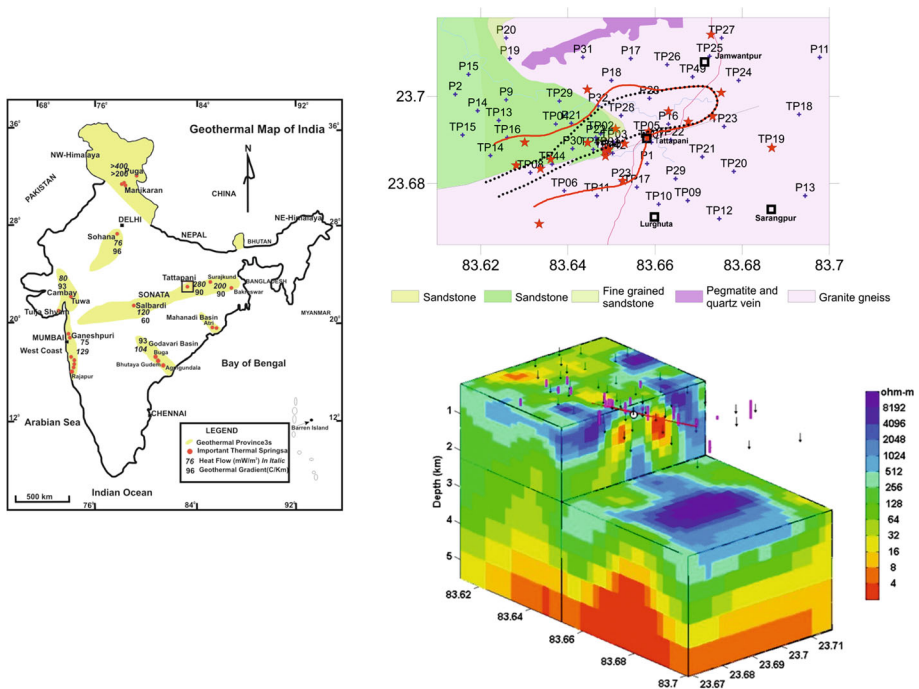
Fig. 28 (Left) Location map of the Tatapani geothermal region. (top) Red contour line represents the boundary of the conductor at 2 km depth level, as obtained from 2D inversion, and the black broken line represents the boundary of the conductor at 1 km depth. (bottom) A longitudinal section through the three-dimensional MT model of Tatapani geothermal region. Red line represents Tatapani fault; black arrow represents MT sites, and boreholes are represented by pink vertical lines
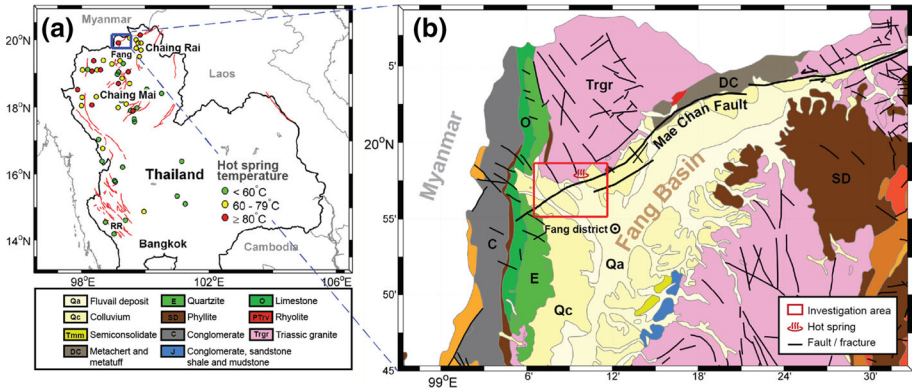
Fig. 29 The regional geology and the location of hot springs are shown (after Amatyakul et al. 2016)
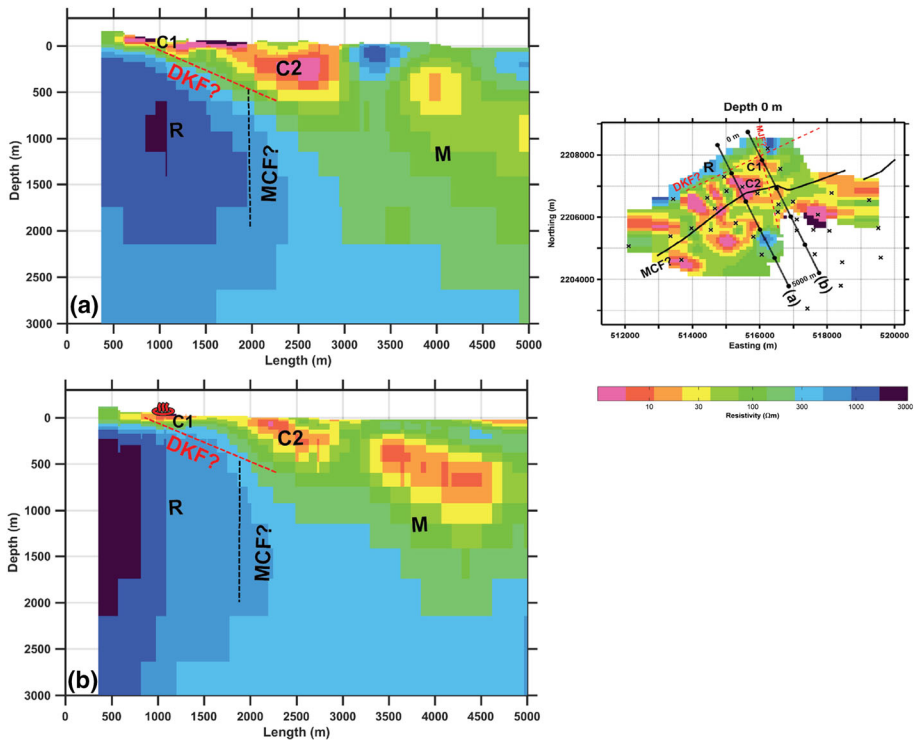
Fig. 30 Vertical cross-section plots of the final inverted model along the profiles a and b. The profile locations are marked on the plot to the right. Black dashed line shows the orientation of the Mae Chan Fault (MCF) (after Amatyakul et al. 2016). The conductor C1 is located below the Fang hot spring and interpreted as clay-rich rock. Conductor C2, which is south of Fang hot spring is interpreted as a promising geothermal reservoir. *DKF* Doi Kia Fault

implementation of rigorous 3D modeling of MT data, cooperative modeling and joint inversion would lead to an effective and successful implementation of any exploration program for exploiting the subsurface target. Further, it is known that porosity and permeability are two important rock parameters that would play a vital role in determining the potential of any geothermal/hydrocarbon target. The relationship between these properties and the electrical resistivity from well log data, calculated from generalized Archie′s law (for, e.g., see Glover 2010; Katz and Thompson 1986; Campanya et al. 2015), would provide deeper insights into the potential of the target area.

Another aspect that needs immediate attention is that, currently, the availability of exploration data and results is rather limited mainly because of the controls enforced by the concerned exploration organizations. Efforts should be made to make the results/data open, to the extent possible so that the academic research community would get an opportunity to have access to such data which in turn would facilitate generating additional contributions that might help further progress in the exploration field and which should be useful to the industry as well.

References

Abdul Azeez KK, Harinarayana T (2007) Magnetotelluric evidence of potential geothermal resource in Puga, Ladakh, NW Himalaya. Curr Sci 93(3):323–329

Abdul Azeez KK, Satish Kumar T, Basava S, Harinarayana T, Dayal AM (2011) Hydrocarbon prospects across Narmada–Tapti rift in Deccan trap, central India: Inferences from integrated interpretation of magnetotelluric and geochemical prospecting studies. Mar Pet Geol 28:1073–1082. doi:10.1016/j.marpetgeo.2011.01.003

Aizawa K, Koyama T, Hase H, Uyeshima M, Kanda W, Utsugi M, Yoshimura R, Yamaya Y, Hashimoto T, Yamazaki K, Komatsu S, Watanabe A, Miyakawa K, Ogawa Y (2014) Three dimensional resistivity structure and magma plumbing system of the Kirishima Volcanoes as inferred from broadband magnetotelluric data. J Geophys Res Solid Earth 119:198–215

Alan W (1969) The crush zone of the Iranian Zagros mountains, and its implications. Geol Mag 106:385–394

Amatyakul P, Arunwan TR, Siripunvaraporn W (2015) A pilot magnetotelluric survey for geothermal exploration in Mae Chan region, northern Thailand. Geothermics 55:31–38

Amatyakul P, Boonchaisuk S, Arunwan TR, Vachiratienchai C, Wood SH, Pirarai K, Fuangswasdi A, Siripunvaraporn W (2016) Exploring the shallow geothermal fluid reservoir of Fang geothermal system, Thailand via a 3-D magnetotelluric survey. Geothermics 64:516–526

Asamori K, Umeda K, Ogawa Y, Oikawa T (2010) Electrical resistivity structure and helium isotopes around Naruko volcano, northeastern Japan and its implication for the distribution of crustal magma. Int J Geophys. doi:10.1155/2010/738139

Austria DCS, Tugawin RJ, Pastor MS, Morillo LB, Banos CFL, Layugan DB (2015) Subsurface characterization of the Leyte geothermal field, Philippines using magnetotellurics. In: Proceedings world geothermal congress, Melbourne, Australia, 19–25 April

Axelsson G, Gunnlaugsson E (2000) Long-term monitoring of high- and low-enthalpy fields under exploitation. International Geothermal Association, World Geothermal Congress 2000 Short Course, Kokonoe, Kyushu District, Japan, p 226

Ayka S, Timur E, Sari C, Caylak C (2015) CSAMT investigations of the Caferbeyli (Manisa/Turkey) geothermal area. J Earth Syst Sci 124:149–159

Bai D, Meju MA, Liao Z (2001) MT images of deep crustal structure of the Rehai geothermal field near Tengchong, Southern China. Geophys J Int 147:677–687

Banos CEFL (1997) 1D interpretation of magnetotelluric data from Southern Leyte geothermal project, Philippines. Geothermal Training Programme, Orkustofnun, Grensasvegur 9, IS-108 Reykjavik, Iceland

Banos CEFL (2012) Three-dimensional magnetotelluric (MT) modelling of the Northern Negros Geothermal Project, Central Philippines. Master of Science thesis, Victoria University of Wellington

Barnett PR, Mandagi S, Iskander T, Abidin Z, Armaladdoss A, Raad R (2015) Exploration and development of the Tawau Geothermal Project, Malaysia. In: Proceedings world geothermal congress, Melbourne, Australia, 19–25 April

Benderitter Y, Cormy G (1990) Possible approach to geothermal research and relative cost estimate. In: Dickson MH, Fanelli M (eds) Small geothermal resources. UNITAR/UNDP Centre for Small Energy Resources, Rome, pp 61–71

Berdichevsky MN, Bubnov V, Aleksanova E, Alekseev D, Yakovlev A, Yakovlev D (2015) Magnetotelluric studies in Russia: regional-scale surveys and hydrocarbon exploration. In: Electromagnetic sounding of the earth's interior, theory, modeling, practice, 2nd edn, pp 379–401. doi:10.1016/B978-0-444-63554-9.00013-1

Berktold A (1983) Electromagnetic studies in geothermal regions. Geophys Surv 6:173–200

Bhattacharya BB, Sinharay RK, Srivastava SV (2003) MT survey over the geothermal region of Bakreshwar for investigation deeper geo-electrical structure. J Geophys 24(1):41–44

Bois C, Bouche P, Pelet R (1982) Global geologic history and distribution of hydrocarbon reserves. Am Asso Petrol Geol Bull 66(9):1248–1270

Campanya J, Jones AG, Vozar J, Rath V, Blake S, Delhaye R, Farrel T (2015) Porosity and permeability constraints from electrical resistivity models: examples using magnetotelluric data. In: Proceedings world geothermal congress 2015, Melbourne, Australia, 19–25, April 2015

Cao Z, He Z, Chang Y (2006) A simulation study of induced polarization effect of magnetotelluric and its application in oil and gas detection. Prog Geophys 21:1252–1257

Chang PY, Lo W, Song SR, Ho KR, Wu CS, Chen CS, Lai YC, Chen HF, Lu HY (2014) Evaluating the Chingshui geothermal reservoir in northeast Taiwan with a 3D integrated geophysical visualization model. Geothermics 50:91–100

Chen Q, Hu W, Li J (2006) Method for inversing real spectral parameters based on magnetotelluric method (MT). J Oil Gas Technol 28:61–64

Chiang CW, Hsu HL, Chen CC (2015) An investigation of the 3D electrical resistivity structure in the Chingshui geothermal area, NE Taiwan. Terr Atmos Ocean Sci 26(3):269–281

Daud Y, Javino F, Nordin MNM, Razak M, Amnan I, Saputra R, Agung L, Sucandra (2010) The first magnetotelluric investigation of the Tawau geothermal prospect, Sabah, Malaysia. In: Proceedings world geothermal congress, Bali, Indonesia, 25–29 April

Davidenko K, Ivanov S, Kudryavceca E, Legeydo P, Veeken PCH (2008) Geo-electric surveying, a useful tool for hydrocarbon exploration: 70th Conference and Exhibition, EAGE, Extended Abstracts, P301

Davydycheva S, Rykhlinski N, Legeydo P (2006) Electrical-prospecting method for hydrocarbon search using the induced-polarization effect. Geophysics 71(4):G179–G189

Dong W, Zhao X (2008) The time-frequency electromagnetic method and its application in western China. Appl Geophys 5(2):127–135

Glover PWJ (2010) A generalized Archie's law for n phases. Geophysics 75(6):E247–E265

GSI 2000 Seismotectonic Atlas of India and Its Environs. Geological Survey of India Publication

Harinarayana T(2008) Application of magnetotelluric studies in India, Memoir Geological Society of India, No. 68, pp 337–356

Harinarayana T, Someswara Rao M, Sarma MVC, Veeraswamy K, Lingaiah A, Prabhakar ER, Virupakshi G, Murthy DN, Sarma SVS (2000a) Magnetotelluric investigations in Tatapani Geothermal region, Surguja district, Madhya Pradesh, India. Technical report, NGRI-2000-exp-282

Harinarayana T, Sastry RS, Nagarajan N, Rao SPE, Manoj C, Naganjaneyulu K, Virupakshi G, Murthy DN, Sarma SVS (2000b) Integrated geophysical studies for hydrocarbon exploration, Kutch, India. NGRI-2000-EXP-296

Harinarayana T, Someswara Rao M, Veeraswamy K, Murthy DN, Sarma MVC, Sastry RS, Virupakshi G, Rao SPE, Patro BPK, Manoj C, Rao M, Sreenivasulu T, Abdul Azeez KK, Naganjaneyulu K, Begum

SK, Kumar BF, Sudha Rani K, Sreenivas M, Prasanth V, Aruna P (2003) Exploration sub-trappean mesozoic basins in the western part of Narmada–Tapti region of Deccan syneclise. NGRI-2003-EXP-404

Harinarayana T, Abdul Azeez KK, Naganjaneyulu K, Manoj C, Veeraswamy K, Murthy DN, Rao SPE (2004) Magnetotelluric studies in Puga valley geothermal field, NW Himalaya, Jammu and Kashmir, India. J Volcanol Geotherm Res 138:405–424

Harinarayana T, Murthy DN, Sudha Rani K, Abdul Azeez KK, Basava S, Roy S, Ray L (2005a) Magnetotelluric and geothermal investigations in Loharinag–Pala hydro power project, Uttaranchal. NGRI technical report no: NGRI-2006- EXP-525

Harinarayana T, Murthy DN, Rao SPE, Sudha Rani K, Srinivasulu T, Abdul Azeez KK, Srinivas M, Virupakshi G (2005b) Magnetotelluric and Geothermal Investigations in Tapovan-Vishnugad hydroelectric power project, Uttaranchal. NGRI technical report no: NGRI-2004-EXP-430

Harinarayana T, Abdul Azeez KK, Murthy DN, Veeraswamy K, Rao SPE, Manoj C, Naganjaneyulu K (2006) Exploration of geothermal structure in Puga geothermal field, Ladakh Himalayas, India by magnetotelluric studies. J Appl Geophys 58:280–295

Harinarayana T, Virupakshi G, Murthy DN, Veeraswamy K, Rao SPE, Abdul Azeez KK, Basava S, Dhanunjaya Naidu G, Shankar R, Sreedhar SV, Sudha Rani K, Gupta AK, Sreenivasulu T, Sreenivas M (2008) Magnetotelluric investigations in geothermal fields of Satluj-Spiti, Beas-Partbati Valleys in Himalchal Pradesh, Badrinath-Tapovan in Uttarakhand and Surajkund in Jharkhand areas, India. NGRI technical report no: NGRI-2008-EXP-637

Harinarayana T, Murthy DN, Sastry RS, Virupakshi SG, Someswara Rao M, Veeraswamy K, Rao SPE, Manoj C, Patro BPK, Abdul Azeez KK, Naganjaneyulu K, Sarma MVC, Srinivasulu T, Basava S, Naidu GD, Gupta AK, Kumara Swamy VTC, Kishore SRK, Phanikiran TV, Ravishankar K, Sreedhar SV, Nageshwara Rao N (2009) Integrated geophysical studies for hydrocarbon exploration in eastern part of the Deccan Syneclise, Central, India. NGRI technical report no: NGRI-2009-EXP-679-Volume II

He Z, Liu H, Tang B (2007) Geoelectrical anomaly patterns of reservoir and geoelectrical methods for direct reservoir detection: 77th Annual International Meeting, SEG, Expanded Abstracts, 698–702

He Z, Hu W, Dong W (2010a) Petroleum electromagnetic prospecting advances and case studies in China. Surv Geophys 31:207–224. doi:10.1007/s10712-009-9093-z

He Z, Hu Z, Luo W, Wang C (2010b) Mapping reservoirs based on resistivity and induced polarization derived from continuous 3D magnetotelluric profiling: case study from Qaidam basin, China. Geophysics 75(1):B25–B33. doi:10.1190/1.3279125

Hochstein MP (1990) Classification and assessment of geothermal resources. In: Dickson MH, Fanelli M (eds) Small geothermal resources. UNITAR/UNDP Centre for Small Energy Resources, Rome, pp 31–59

Hoversten GM, Cassassuce F, Gasperikova E, Newman GA, Chen J, Rubin Y, Hou Z, Vasco D (2006) Direct reservoir parameter estimation using joint inversion of marine seismic AVA and CSEM data. Geophysics 71(3):C1–C13. doi:10.1190/1.2194510

Ichinoseki H (1984) Exploration and development of the Yurihara oil and gas field. J Jpn Assoc Petrol Technol 49:226–233 (in Japanese)

Katz AJ, Thompson AH (1986) Quantitative prediction of permeability in porous rock. Phys Rev B 34:8179–8181

Kaya C, Basokur AT (2010) Magnetotelluric experiments in the Aliaga geothermal field, Western Turkey. In: Proceedings world geothermal congress, Bali, Indonesia, 25–29

Komori S, Utsugi M, Kagiyama T, Inoue H, Chen CH, Chiang HT, Chao BF, Yoshimura R, Kanda W (2014) Hydrothermal system in the Tatun Volcano Group, northern Taiwan, inferred from crustal resistivity structure by audio-magnetotellurics. Prog Earth Planet Sci 1:20

Krishna VG, Rao NM, Sarkar D (1999) The problem of velocity inversion in refraction seismics: some observations from modelling results. Geophys Prospect 47:341–357

Lashin A, Arifi NA (2014) Geothermal energy potential of southwestern of Saudi Arabia "exploration and possible power generation": a case study at Al Khouba area—Jizan. Renew Sustain Energy Rev 30:771–789

Lashin A, Pipan M, Arifi NA, Bassam AA, Mocnik A, Forte E (2015) Geophysical exploration of the Western Saudi Arabian Geothermal province: first results from the Al-Lith Area. In: Proceedings world geothermal congress, Melbourne, Australia, 19–25 April

Layugan DB, Rigor DM, Apuada NA Jr, Banos CFL, Olivar RER (2005) Magnetotelluric (MT) Resistivity surveys in various geothermal systems in Central Philippines. In: Proceedings world geothermal congress, Antalya, Turkey, 24–29 April

Lee TJ, Song Y, Uchida T, Mitsuhata Y, Oh S (2004) Interpretation of 3D magnetotelluric data including sea effect for geothermal exploration in Pohang, Korea. In: Proceedings of the 6th Asian geothermal symposium, 26–29 October, mutual challenges in high and low temperature geothermal resource fields, pp 139–143

Lee TJ, Song Y, Uchida T (2007) Three dimensional magnetotelluric surveys for geothermal development in Pohang, Korea. Explor Geophys 38:89–97

Lee TJ, Han N, Song Y (2010) Magnetotelluric survey applied to geothermal exploration: an example at Seokmo Island, Korea. Explor Geophys 41:61–68

Lee TJ, Song Y, Park DW, Jeon J, Yoon WS (2015) Three dimensional geological model of Pohang EGS Pilot Site, Korea. In: Proceedings world geothermal congress, Melbourne, Australia, 19–25 April

Leeuwen WAV, Marnette K, Schotting RJ, Muller M (2015) A geothermal exploration MT data set and its 3D inversion using two different codes: an example from Western Turkey. In: Proceedings world geothermal congress, Melbourne, Australia, 19–25 April

Mansoori I, Oskooi B, Pederson L (2015) Magnetotelluric signature of anticlines in Iran's Sehqanat oil field. Tectonophysics 654:101–112

Mansoori I, Oskooi B, Pederson L, Javaheri R (2016) Three-dimensional modelling of magnetotelluric data to image Sehqanat hydrocarbon reservoir in southwestern Iran. Geophys Prospect 64:753–766

Maryanto S, Wicaksono AS, Santoso DR, Nadhir A, Gunawah H, Prasodjo E, Suantika IG (1992) Multi geosciences approach at Blawan-Ijen Volcano-Geothermal Complex, East Java, Indonesia to Understand it utilization and hazard. In: Goldschmidt conference

Matsuo K, Negi T (1999) Oil exploration in the difficult Minami-Noshiro area part 2: Magnetotelluric survey. Lead Edge 18:1411–1413

Meju MA (2002) Geoelectromagnetic exploration for natural resources: models, case studies and challenges. Surv Geophys 23:133–205

Merh SS (1995) Geology of Gujarat. Geological Society of India, Bangalore, pp 1–222

Mitsuhata Y, Matsuo K, Minegishi M (1999) Magnetotelluric survey for exploration of a volcanic-rock reservoir in the Yurihara oil and gas field, Japan. Geophys Prospect 47:195–218

Muffler P, Cataldi R (1978) Methods for regional assessment of geothermal resources. Geothermics 7:53–89

Munoz G (2014) Exploring for geothermal resources with electromagnetic methods. Surv Geophys 35:101–122

Mustopa EJ, Furuya S, Jotaki H, Ushijima K (2002) Application of magnetotelluric method to Takigami geothermal field in Kyushu, Japan. Memories of the Faculty of Engineering, Kyushu University, vol 62(4)

Niasari SW, Munoz G, Kholid M, Suhanto E, Ritter O (2012) Magnetotelluric exploration of the Sipoholon geothermal field, Indonesia. 24 Schmucker-Weidelt-Kolloquium, Neustadt an der Weinstra Be, 19–23 September

Nicholson KN (1993) Geothermal fluids. Chemistry and exploration techniques. Springer, Berlin

Nurhasan Ogawa Y, Ujihara N, Tank SB, Honkura Y, Onizawa S, Mori T, Makino M (2006) Two electrical conductors beneath Kusatsu–Shirane volcano, Japan, imaged by audiomagnetotellurics, and their implications for the hydrothermal system. Earth Planet Space 58:1053–1059

Ogawa Y, Ichiki M, Kanda W, Mishina M, Asamori K (2014) Three-dimensional magnetotelluric imaging of crustal fluids and seismicity around Naruko volcano, NE Japan. Earth Planets Space 66:158

Oskooi B, Darijani M (2013) 2D inversion of the magnetotelluric data from Mahallat geothermal field in Iran using finite element approach. Arab J Geosci. doi:10.1007/s12517-013-0893-6

Oskooi B, Mirzaei M, Mohannadi B, Mohammadzadeh-Moghaddam M, Ghadimi F (2016) Integrated interpretation of the magnetotelluric and magnetic data from Mahallat geothermal field, Iran. Stud Geophys Geod 60:141–161. doi:10.1007/s11200-014-1235-1

Ozawa A, Katahira T, Nakano S, Tsuchiya N, Awata Y (1988) Geology of the Yashima district, with Geological Sheet Map at 1:50,000. Geological Survey of Japan, pp 87 **(in Japanese with English abstract)**

Pandey D, MacGregor L, Sinha M, Singh S (2008) Feasibility of using the magnetotelluric method for subbasalt imaging at Kachchh, India. Appl Geophys 5(1):74–82. doi:10.1007/s11770-008-0008-4

Pandey D, Singh S, Sinha M, MacGregor L (2009) Structural imaging of Mesozoic sediments of Kachchh, India and their hydrocarbon prospects. Mar Pet Geol 26:1043–1050

Parnadi WW, Widodo Savitri RW, Zakarsyi A (2014) Magnetotelluric investigations in the way Umpu geothermal prospect area, Lampung province, Indonesia. Int J Technol 3:227–241

Patro BPK, Sarma SVS (2007) Trap thickness and the subtrappean structures related to mode of eruption in the Deccan plateau of India: results from magnetotellurics. Earth Planet Space 59:75–81

Patro PK, Abdul Azeez KK, Veeraswamy K, Sarma SVS, Sen MK (2015a) Sub-basalt sediment imaging—the efficacy of magnetotellurics. J Appl Geophys 121:106–115. doi:10.1016/j.jappgeo.2015.07.010

Patro PK, Rao SPE, Reddy KC, Raju K, Borah UK, Sana S, Sarma SVS (2015b) Re-evaluation of the deep electrical structure of Tattapani hot spring area using advanced MT data analysis and 3D modelling approaches. Technical report no. NGRI-2015-EXP-896

Pellerin L, Johnston JM, Hohmann GW (1996) A numerical evaluation of electromagnetic methods in geothermal exploration. Geophysics 61:121–130

Raharjo IB, Maris V, Wannamaker PE, Chapman DS (2010) Resistivity structures of Lahendong and Kamojang geothermal systems revealed from 3D magnetotelluric inversions, a comparative study. In: Proceedings, world geothermal congress, Bali, Indonesia, 25–29 April

Rao SPE, Naidu GD, Harinarayana T, Sarma SVS, Gupta AK (2014) An anomalous high conductivity upper crustal body detected underneath the Surajkund hot spring area from a magnetotellric study. J Indian Geophys Union 18(4):425–433

Reyes AN (1999) Interpretation of Schlumberger and magnetotelluric measurements: examples from the Philippines and Iceland. Geothermal Training Programme, Orkustofnun, Grensasvegur 9, IS-108 Reykjavik, Iceland

Rezaie AH, Nogole Sadat MA (2004) Fracture modeling in Asmari reservoir of Rag-e Sefid oil field by using multi well image log (FMS/FMI). Iran Int J Sci 5(1):107–121

Rosario RAD Jr, Oanes AF (2010) Controlled source magnetotelluric survey of Mabini geothermal prospect, Mabini, Batangas, Philippines. In: Proceedings world geothermal congress, Bali, Indonesia, 25–29 April

Rosario RAD Jr, Pastor MS, Malapitan RT (2005) Controlled source magnetotelluric (CSMT) survey of Malabuyoc thermal project, Malabuyoc/Alegria, Cebu, Philippines. In: Proceedings world geothermal congress, Antalya, Turkey, 24–29 April

Sarma SVS, Harinarayana T, Gupta ML, Sarma SR, Kumar R, Sanker Narayan PV (1983) A reconnaissance telluric survey in northern parts of Konkan geothermal province, India. Geophys Res Bull 21(1):91–99

Sarma SVS, Virupakshi G, Murthy DN, Harinarayana T, Sastry TS, Rao MS, Nagarajan N, Veeraswamy K, Sarma MS, Rao SPE, Gupta KRB (1992) Magnetotelluric studies for oil exploration over Deccan Traps, Saurashtra, Gujarat, India. NGRI-92-LITHOS-125

Sarma SVS, Virupakshi G, Harinarayana T, Murthy DN, Someswara Rao M, Sastry RS, Nagarajan N, Sastry TS, Sarma MVC, Rao M, Veeraswamy K, Rao SPE, Gupta KRB, Lingaiah A, Sreenivasulu T, Raju AVSN, Patro BPK, Manoj C, Bansal A, Kumaraswamy VTC, Sannasi SR, Stephen C, Naganjaneyulu K (1998a) Integrated geophysical studies for hydrocarbon exploration Saurashtra, India. NGRI-98-EXP-237

Sarma SVS, Virupakshi G, Harinarayana T, Rao M, Nagarajan N, Someswara Rao M, Sastry TS, Rao SPE, Gupta KRB, Patro BPK, Raju AVSN, Jyoti RS, Srinivasulu T, Lingaiah A (1998b) Magnetotelluric studies in Nagpur-Wardha area. NGRI technical report no: NGRI-98-EXPL-222

Sarma SVS, Virupakshi G, Harinarayana T, Nagarajan N, Someswara Rao M, Murthy DN, Veeraswamy K, Rao M, Rao SPE, Sastry TS, Patro BPK, Raju AVSN, Lingaiah A, Srinivasulu T, Naganjaneyulu K (1998c) Magnetotelluric studies along Nagpur—Belgaum and Morsi-Akot-Harda Profiles. NGRI technical report no: NGRI-98-EXPL-234

Sarvandani MM, Kalateh AN, Unsworth M, Majidi A (2017) Interpretation of magnetotelluric data from the Gachsaran oil field using sharp boundary inversion. J Petrol Sci Eng 149:25–39. doi:10.1016/j.petrol.2016.10.019

Satpal Singh OP, Sar D, Chatterjee SM, Sawa S (2006) Integrated interpretation for sub-basalt imaging in Saurashtra Basin, India. Lead Edge 25:882–885

Seki K, Kanda W, Ogawa Y, Tanbo T, Kobayashi T, Hino Y, Hase H (2015) Imaging the hydrothermal system beneath the Jigokudani valley, Tateyama volcano, Japan: implications for structures controlling repeated phreatic eruptions from an audio-frequency magnetotelluri survey. Earth Planet Space 67(6):6

Seki K, Kanda W, Tanbo T, Ohba T, Ogawa Y, Takakura S, Kenji N, Ushioda M, Suzkuki A, Saito Z, Matsunaga Y (2016) Resistivity structure and geochemistry of the Jigokudani Valley hydrothermal system, Mt. Tateyama. Jpn J Volcanol Geotherm Res 325:15–26. doi:10.1016/j.jvolgeores.2016.06.010

Singh B, Arora K (2008) Geophysical exploration for petroleum in the Subtrappean Mesozoic sedimentary formations of India. Mem Geol Soc India 68:237–258

Sinharay RK, Srivastava S, Bhattacharya BB (2001) An analysis of magnetotelluric (MT) data over geothermal region of Bakreshwar, West Bengal. J Geophys 22(1):31–39

Sinharay RK, Srivastava S, Bhattacharya BB (2010) Audiomagnetotelluric studies to trace the hydrological system of thermal fluid flow of Bakreswar Hot Spring, Eastern India: a case history. Geophysics 75(5):B187–B195

Sircar A, Shah M, Sahajpal S, Vaidya D, Dhale S, Chaudhary A (2015) Geothermal exploration in Gujarat: case study from Dholera. Geotherm Energy 3:22

Song Y, Lee SK, Kim HC, Kee WS, Park YS, Lim MT, Son JS, Cho SJ, Lim SK, Uchida T, Mitsuhata Y, Lee TJ, Lee H, Rim HR, Hwang S, Park IH (2003) Case study on a low enthalpy geothermal exploration in Pohang Area, Korea. Geosyst Eng 6(2):46–53

Spichak VV (2005) Three-dimensional resistivity structure of the Minamikayabe geothermal zone revealed by Bayesian inversion of MT data. In: Proceedings world geothermal congress, Antalya, Turkey, 24–29 April

Spichak VV, Manzella A (2009) Electromagnetic sounding of geothermal zones. J Appl Geophys 68:459–478

Strack KM (2014) Future directions of electromagnetic methods for hydrocarbon applications. Surv Geophys 35:157–177. doi:10.1007/s10712-013-9237-z

Strack KM, Pandey PB (2007) Exploration with controlled-source electromagnetic under basalt cover in India. Lead Edge 26:360–363

Sui XW, Zhang J, Shi FJ, Zhao JC (2011) Evaluation on the geothermal resources in Jingbo Lake Graben of the Dun-Mi Fault Zone in Helongjiang Province. Geoscience 25:377–383 **(In Chinese)**

Sumintadireja P, Saepuloh A, Irawan D, Junursyah L (2011) Temporal analysis of visible-thermal infrared band and magnetotelluric method to simulate a geothermal sitting at Mt. Ciremai, West Java, Indonesia. In: Proceedings, thirty sixth workshop on geothermal reservoir engineering, Stanford University, Stanford, California, January 31–February 2

Takin M (1972) Iranian geology and continental drift in the Middle East. Nature 235:147–150

Tuyen DV, Vu TA, Phong LH, Dat PN, Toan DV, Si LV (2015) Structural features of geothermal field from magnetotelluric survey in Northern Central Region of Vietnam. In: Proceedings world geothermal congress, Melbourne, Australia, 19–25 April

Uchida T (1993) Smooth 2D inversion for magnetotelluric data based on statistical criterion ABIC. J Geomagn Geoelectr 45:841–858

Uchida T (2003) Application of 3D Inversion to magnetotelluric data in the Ogiri Geothermal Area, Japan. Geotherm Resour Counc Trans 27:12–15

Uchida T (2005) Three dimensional magnetotelluric investigation in geothermal fields in Japan and Indonesia. In: Proceedings world geothermal congress, Antalya, Turkey, 24–29 April

Uchida T, Ogawa Y (1993) Development of FORTRAN code of two-dimensional magnetotelluric inversion with smoothness constraint. Geological survey of Japan, open-file report no. 205, p 115

Uchida T, Song Y, Lee TJ, Mitsuhata Y, Lim SK, Lee SK (2005) Magnetotelluric survey in an extremely noisy environment at the Pohang low enthalpy geothermal area, Korea. In: Proceedings world geothermal congress, Antalya, Turkey, 24–29 April

Uchida T, Takakura S, Ueda T, Adachi M, Ozeki H, Kamada K, Sato T (2011) 3D magnetotelluric survey at the Yanaizu-Nishiyama geothermal field, Northen Japan. In: Proceedings of the 9th Asian geothermal symposium, 7–9 November

Umeda K, Asamori K, Negi T, Ogawa Y (2006) Magnetotelluric imaging of crustal magma storage beneath the Mesozoic crystalline mountains in a nonvolcanic region, northeast Japan. Geochem Geophys Geosyst 7:Q08005. doi:10.1029/10052006GC001247

Unsworth M (2005) New developments in conventional hydrocarbon exploration with electromagnetic methods. Can Soc Explor Geophys Rec 30(4):34–38

Ushijima K, Mustopa EJ, Jotaki H, Mizunaga H (2005) Magnetotelluric soundings in the Takigami geothermal area, Japan. In: Proceedings world geothermal congress, Antalya, Turkey, 24–29 April

Waseda A, Omokawa M (1990) Generation, migration and accumulation of hydrocarbons in the Yurihara oil and gas field. J Jpn Assoc Petrol Technol 55:233–244 **(in Japanese with English abstract)**

Wright PM, Ward SH, Ross HP, West RC (1985) State of the art geophysical exploration for geothermal resources. Geophysics 50:2666–2696

Wu G, Hu X, Huo G, Zhou X (2012) Geophysical exploration for geothermal resources: an application of MT and CSAMT in Jiangxia, Wuhan, China. J Earth Sci 23(5):757–767

Yamane K, Ohsato K, Ohminato T, Kim HJ (2000) Three dimensional magnetotelluric investigation in Kakkonda geothermal area, Japan. In: Proceedings world geothermal congress, Kyushu-Tohoku, Japan, May 28–June 10

Zakharova OK, Spichak VV, Rybin AK, Batalev VY, Goidina AG (2007) Estimation of the correlation between magnetotelluric and geothermal data in the Bishkek geodynamic research area, Izvestiya. Phys Solid Earth 43(4):35–42

Zarkasyi A, Rahadinata T, Suhanto E, Widodo S (2015) Investigation of geothermal structures of the Kadidia Area, Indonesia, using the magnetotelluric method. In: Proceedings world geothermal congress, Melbourne, Australia, 19–25 April

Zhang K, Wei W, Lu Q, Dong H, Li Y (2014) Theoretical assessment of 3-D magnetotelluric method for oil and gas exploration: synthetic examples. J Appl Geophys 106:23–36

Zhang L, Hao T, Xiao Q, Wang J, Zhou L, Qi M, Cui X, Cai N (2015) Magnetotelluric investigation of the geothermal anomaly in Hailin, Mudanjiang, northeastern China. J Appl Geophys 118:47–65

Ziolkowski A, Hobbs B, Wright D (2002) First direct hydrocarbon detection and reservoir monitoring using transient electromagnetic. First Break 20:224–225

Ziolkowski A, Hanssen P, Gatliff R, Jakubowicz H, Dobson A, Hampson G, Li X, Liu E (2003) Use of low frequencies for sub-basalt imaging. Geophys Prospect 51(3):169–182

Zonge KL, Sauck WA, Sumner JS (1972) Comparison of time, frequency and phase measurements in induced polarization. Geophys Prospect 20:626–648

Zutshi PL (1991) The Deccan Trap-its implication on hydrocarbon exploration in western India. Bull Oil Nat Gas Commun 28(2):90–95